Journal of
Hydroinformatics

Journal of Hydroinformatics Vol 26 No 9, 2325 doi: 10.2166/hydro.2024.130

Surface water dynamics of Lake Chad Basin (Sahelian Africa) based on daily temporal resolution Earth observation time series

Reeves M. Fokeng [a,*], Felix Bachofer [a], Patrick Sogno [a], Igor Klein [a], Soner Uereyen [a] and Claudia Kuenzer [a,b]

[a] German Remote Sensing Data Center (DFD), German Aerospace Center (DLR), Wessling, Germany
[b] Department of Remote Sensing, Institute of Geography and Geology, University of Wuerzburg, Wuerzburg, Germany
*Corresponding author. E-mail: meli.fokeng@dlr.de

RMF, 0000-0002-6303-2128; FB, 0000-0001-6181-0187; PS, 0000-0001-7474-4035; IK, 0000-0003-0113-8637; SU, 0000-0003-3733-0049

ABSTRACT

Water availability is vital for the sustenance of livelihoods in the Lake Chad Basin. However, the daily and seasonal dynamics of open water bodies are not well understood. This study aims to (1) analyze the daily and seasonal dynamics of water bodies, (2) estimate changes in surface water area extent including trends and change points, and (3) assess the connection between surface water extent and seasonal rainfall variation. To achieve this, we used the Global WaterPack and ERA5-Land daily aggregated datasets. We employed time series decomposition, trends analysis, and temporal lag correlation in our analysis. The results showed strong seasonal patterns of natural lakes compared to reservoirs/dams. Between 2003 and 2022, Lake Chad averaged 2,475.64 km^2. The Northern pool of Lake Chad exhibited significant fluctuations, remaining below 600 km^2 between 2005 and 2012, from 2016 to 2019), with less than 350 km^2 lasting only for a few days annually. The Southern pool averaged between 2,200 and 2,400 km^2, except during drought years (2006–2007), specifically between the days of the year to approximately 66, and days 301–365/6. In Lake Fitri, the yearly maximum and minimum water extents were observed between days 1–59 and 305–365/6, and between days 60 and 304, respectively.

Key words: change points, daily surface water duration, Earth observation, Global WaterPack, Lake Chad

HIGHLIGHTS

- Natural lakes exhibit strong seasonal contrasts as opposed to reservoirs/dams.
- Open surface water bodies show monotonic or cyclic patterns.
- Several phases of dwindling and recovery were identified in Lake Chad's cycle.
- Lake Chad currently exists as '*small Lake Chad*' with a highly fluctuating Northern pool.
- Open surface water bodies variably respond to seasonal rainfall variation.

GRAPHICAL ABSTRACT

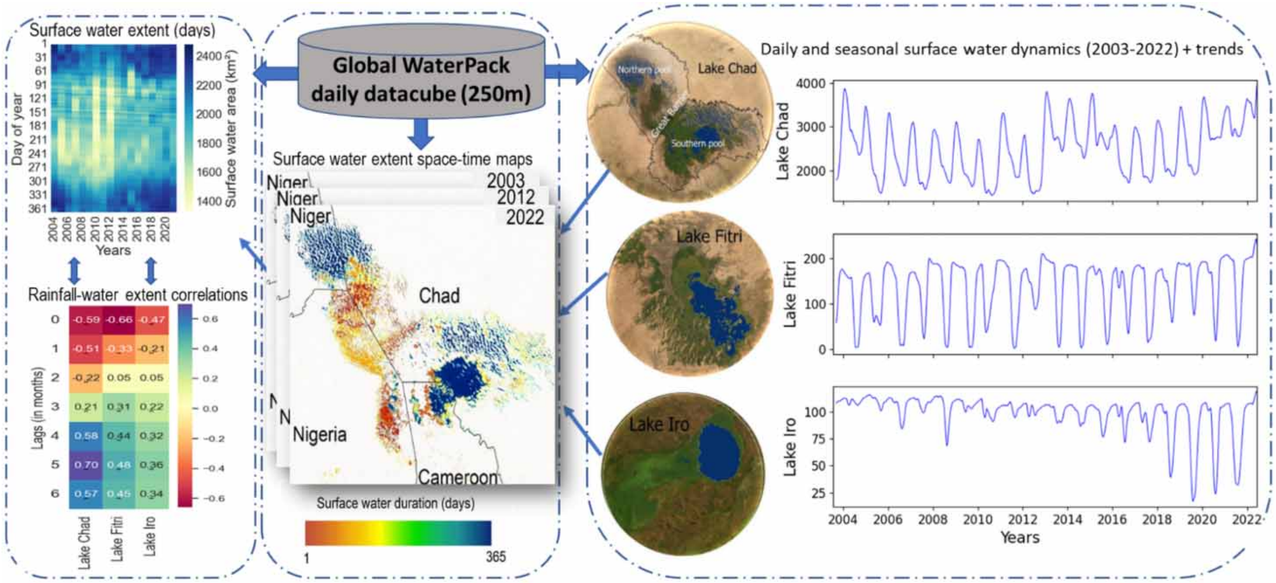

ABBREVIATIONS

BGR	Federal Institute for Geosciences and Natural Resources
DOY	Day of year
EO	Earth observation
FAO	Food and Agriculture Organization of the United Nations
GIZ	The German Agency for International Cooperation (Deutsche Gesellschaft für Internationale Zusammenarbeit)
GWP	Global WaterPack
GWSP IPO	Global Water System Project International Project Office
HVIP	Hadejia Valley Irrigation Project
JRC	Joint Research Centre
KRIP	Kano River Irrigation Project
LCB	Lake Chad Basin
LCBC	Lake Chad Basin Commission
MK/MMK	Mann–Kendall/modified Mann–Kendall
UNESCO	United Nations Educational, Scientific and Cultural Organization

1. INTRODUCTION

Climate change is affecting ecosystems and livelihoods across the globe today, with profound impacts on freshwater resources, and corresponding effects on basin-scale livelihoods. The Lake Chad Basin (LCB) of Sahelian Africa is facing a stroke of environmental and political crises exacerbated by armed conflicts and mishandling of land resources. While home to 49 million people (FAO 2021), Lake Chad constitutes a UNESCO World Heritage and Ramsar site. During the last decades, drought and anthropogenic influences have led to the diminishment of Lake Chad with adverse effects on both food and water resources (Birkett 2000; Candela *et al.* 2014). Between 1950 and 1970, the area covered by open waters and swamps decreased by three; from around 25,000 km^2 in the 1960s to less than 2,500 km^2 in recent years (FAO 2009; LCBC 2016; Hansen 2017). Recent studies by GIZ (2018), Vivekananda *et al.* (2019), Pham-Duc *et al.* (2020) and Gbetkom *et al.* (2023) show increasing rainfall over the Sahel leading to somewhat stability of the lake's extent, despite the highly fluctuating nature of its Northern pool. An understanding of hydrological dynamics of Sahelian watersheds is a priority in the face of climate change and demographic explosion. As a result of environmental dynamism in the basin, Lake Chad became divided into Northern and Southern pools around July 1973 (Olivry 1996), separated by a Great Barrier (Lemoalle & Magrin 2014), covered by a continuous stretch of vegetation (see Figure 1(a)).

(a)

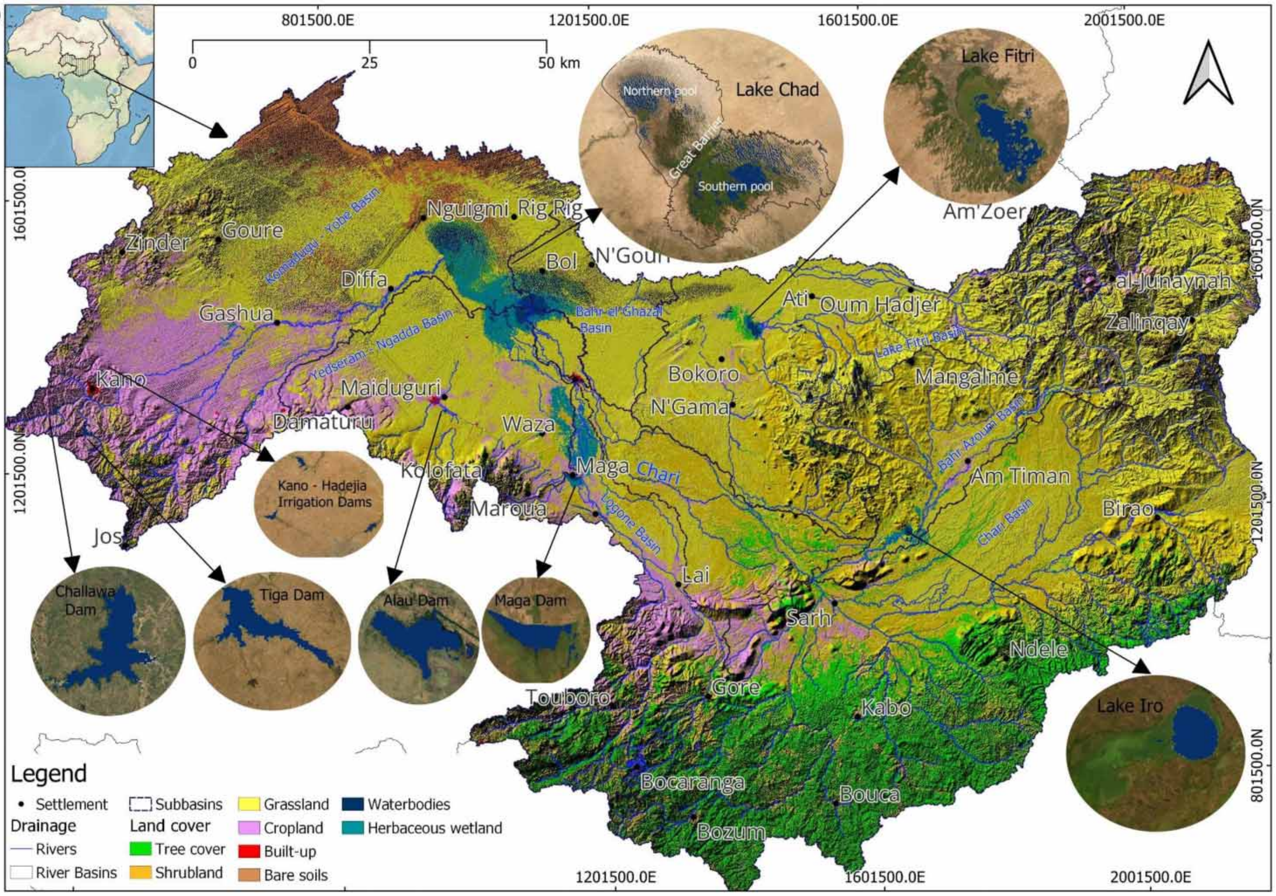

Figure 1 | (a) Geographical setting of the LCB, land cover (Zanaga *et al.* 2021), and topographic configuration (European Union Copernicus Programme 2021). (b) Methodological flowchart of the study. (*continued.*).

The Southern pool is further segmented into zones of open water and archipelagoes. While the Northern pool contains mostly seasonal water, the Southern pool remains quasi-stable but fluctuates between wet and dry episodes. Despite recent increases in precipitation over the basin, the lake does not completely recover due to groundwater level decline, population pressure, and reduced discharges (Geerken *et al.* 2012). Whilst freshwater resources remain vital for sustenance in semi-arid and arid areas, water resources management is already hard hit by climate change. Therefore, global monitoring and knowledge of spatial and temporal variability of surface water resources are of high importance (Klein *et al.* 2021b).

Despite the plethora of studies in LCB, scientific knowledge on surface water duration on a daily time scale is still not documented. Many studies on climate variability and hydrological shifts have been conducted (Wald 1990; De Zborowski & Lemoalle 1996; Birkett 2000; Coe & Birkett 2004; Gao *et al.* 2011; Candela *et al.* 2014; Okonkwo *et al.* 2014; Zhu *et al.* 2017; Buma *et al.* 2018; Pattnayak *et al.* 2019; Pham-Duc *et al.* 2020; Mahamat Nour *et al.* 2021; Fu *et al.* 2023; Gbetkom *et al.* 2023; Lemenkova 2023). While most studies have focused on Lake Chad (Zhao *et al.* 2023), fewer studies have attempted to understand dynamics in other open water bodies within the basin, as demonstrated by (Djimadoumngar & Adegoke 2018; Poulin *et al.* 2019; Abba Umar *et al.* 2021; Christine *et al.* 2021). Most previous studies (Coe & Birkett 2004; Lemoalle 2004; Gao *et al.* 2011; Lemoalle & Magrin 2014; Okonkwo *et al.* 2014; Buma *et al.* 2018; Pham-Duc *et al.* 2020; Gbetkom *et al.* 2023) employ satellite altimetry in the study of lake water dynamics. How dense time series derived from optical remote sensing could help reconstruct surface water dynamics is not well documented. Also, not only the seasonal patterns of open water resources are not fully understood, but scientific details on their daily dynamics are completely missing in the research landscape. The extent to which daily and seasonal surface water varies with precipitation is also not fully understood. According to the Food and Agricultural Organization (FAO), one main problem of the LCB is the variability of the hydrological regime and the dramatic decrease in freshwater availability (FAO 2009).

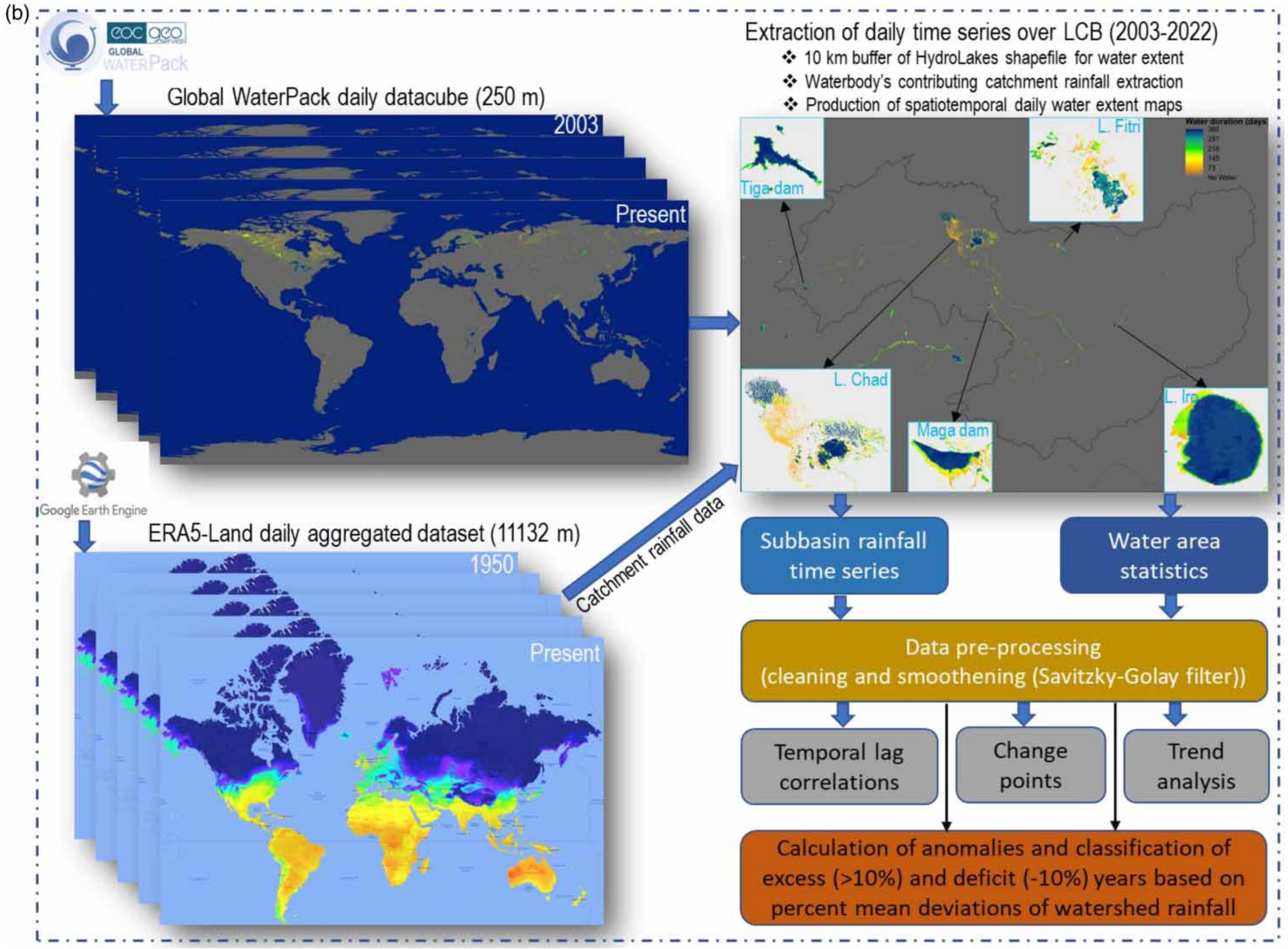

Figure 1 | Continued.

The advancements in remote sensing in the past decades have enabled large-scale and long-term analyses to reconstruct land surface dynamics amongst others. As such, powerful methods and tools have been developed for analyzing Earth observation (EO) data (Klein *et al.* 2017). Several studies (Klein *et al.* 2014, 2015; Mueller *et al.* 2016; Pekel *et al.* 2016; Zhou *et al.* 2017; Huang *et al.* 2018; Li *et al.* 2020; Ling *et al.* 2020; Pickens *et al.* 2020; Bonnema *et al.* 2022; Liu *et al.* 2022; Yang *et al.* 2022) have demonstrated such space-based estimation of open surface water dynamics using dense EO data. We employed a temporally dense, daily cloud and gap-free global dataset on water bodies' dynamics, the Global WaterPack (GWP) (Klein *et al.* 2024, 2021a, 2017; Uereyen *et al.* 2022) for reconstructing the daily and seasonal patterns of open water bodies in the most active part of the LCB. The GWP is derived from daily remote sensing image time series at a spatial resolution of 250 m using a dynamic thresholding methodology that captures rapid changes in surface water extent at a high temporal frequency (Klein *et al.* 2024).

The objectives of this study are: (1) to analyze the daily and seasonal dynamics of open surface water in the LCB, (2) to estimate change in open surface water area extent, including trends and change points, and (3) to assess the relationship between surface water extent and seasonal rainfall variation in the basin. Our study represents a significant contribution to the hydrological balance of the lake system as it focuses on the daily and detailed seasonal surface water dynamics. Unlike previous studies that analyze long-term trends, this study provides a granular view of how the water bodies' surface extent fluctuates daily and seasonally derived based on medium spatial resolution remote sensing data. This work not only improves our knowledge of the basin's hydrology but also provides vital information for real-time resource management and landscape planning in the context of climate change.

2. MATERIALS AND METHODS

2.1. The Lake Chad Basin

Lake Chad is an endorheic lake in Sahelian Africa, with an extension to hyper-arid areas of the Tibesti Mountains. The most vegetative part of the LCB constitutes the southern portion (Figure 1(a)). Open surface water bodies and groundwater offer better opportunities for rain-fed agriculture for over 60% of the population (Vaquero *et al.* 2021) in LCB. Both surface and groundwater variations in the LCB are not fully understood. The lake is sourced by two main contributing areas, the Chari-Logone and the Komadugu-Yobe headwaters, direct surface rainfall, and groundwater flows. According to Bader *et al.* (2011) and GIZ (2018), the Komadugu-Yobe Basin contributes 1.8–2% of the flow to Lake Chad.

The Chari River rising from the southern ridge contributes more than 80–95% (GIZ 2018)) of the lake's water while surface rainfall contributes 15% (Olivry 1996), mostly as runoff from the southwestern section. The lake's water cycle is rhythmed by monsoon with minimum levels around April–May and maximum levels around December–January (Bader *et al.* 2011), thus exhibiting a significant lag between rainfall and lake surface water area. Vaquero *et al.* (2021) established that most rainfall occurs between April and October, while potential evapotranspiration (PET) values of 2,000–3,000 mm/year are common. Precipitation rates vary from an average of 1,400 mm/year in the south to 10 mm/year in the north (Global Water Partnership 2013). With a mostly flat topography, runoff is only produced along the basin's southern periphery, making groundwater a vital component in the preservation of Lake Chad (Geerken *et al.* 2012; GWSP IPO 2012).

Surface flow in the LCB is mostly ephemeral, with the exception of rivers Komadugu-Yobe and Ebeji (El-Beïd) (Figure 1(a)) in the southwestern section (Goni *et al.* 2021), and rivers Logone and Chari from the southeastern section that drains directly into Lake Chad (Goni *et al.* 2021). Goni *et al.* (2021) found this to be linked to the basin's geological setting; deeply weathered crystalline rocks. The underlying geological setting of the lake's basin, mostly a succession of marine and continental sediments deposited on the Precambrian basement of the Mesozoic (Cretaceous), Cenozoic and Quaternary (Vaquero *et al.* 2021), makes it an excellent reservoir for groundwater. BGR (n.d.) reported that 11,395 boreholes tap groundwater from the Quaternary aquifer of the basin.

2.2. Datasets and pre-processing

In this study, we employed the GWP (Klein *et al.* 2017, 2024), a daily time series of open surface water dynamics for the period 2003–2022. The GWP dataset is produced by using a pixel-based water classification approach based on dynamical thresholding and temporal interpolation (Klein *et al.* 2021b), consisting of daily open water/no water layers which were generated by the combination of one-class classifications derived from the latest Moderate Resolution Imaging Spectroradiometer (MODIS) reflectance products of the Terra (MODGQ09) and Aqua (MYDGQ09) satellites of the same day (Klein *et al.* 2021a, 2021b). Details on data quality and accuracy can be found in Klein *et al.* (2017, 2021b, 2024).

For this research, we selected open water bodies above 10 km^2 area using HydroLAKES shapefile (Messager *et al.* 2016). These include Lake Chad, Lake Fitri, Lake Iro, Maga Dam, Alau Dam, Tiga Dam, Challawa Dam, Wattari Dam, Kano River Irrigation Project (KRIP), and Hadejia Valley Irrigation Project (HVIP) (Figure 1(a)). We prepared a 10 km buffer (here seen as the approximate maximum extent of surface water during flood events) for each water body's shapefile and used it to extract the zonal statistics and construct the daily time series. To reduce outliers and get a smoothened time series of GWP, we decomposed the time series into trends, seasonality and residuals/noise components using an additive model. At a later stage, we used the Savitzky-Golay filter (Savitzky & Golay 1964), window length = 50 and polyorder = 3 to smoothen the residuals, before recomposing (trend, seasonality and cleaned residuals) to get a cleaner time series from 2003 to 2022 (Figure 1(b)).

Further, we acquired and processed ERA5-Land reanalysis dataset (Muñoz-Sabater *et al.* 2021) via Google Earth Engine (Gorelick *et al.* 2017), for daily precipitation (rainfall) time series (2003–2022) the same way as GWP (Figure 1(b)). Spatio-temporal maps of open surface water duration and extent for all water bodies with an area above 100 km^2 were produced.

2.3. Trend analysis

Trend analysis of remote sensing time series (Dubovyk *et al.* 2013) is vital for determining trends and direction of change patterns. Different methods exist, e.g. the Mann–Kendall (MK), Modified Mann–Kendall (MMK), and Cox–Stuart tests for detecting trends (Militino *et al.* 2020; Fu *et al.* 2023). The Theil–Sen Slope (Theil 1950; Sen 1968) calculates the magnitude of the trend observed in the data. It calculates the magnitude of a monotonous trend as the median of the slopes (β_i) of the lines through all point pair combinations (x_j and x_i are the data values at times j and i, with $j > i$) (Eisfelder *et al.* 2023):

$$\beta_i = \frac{x_j - x_i}{j - i} \text{ for } i, \ldots, n \tag{1}$$

where $1 < j < i < n$, when $\beta_i > 0$, it implies an increasing trend; when $\beta_i < 0$, it implies a decreasing trend (Fu *et al.* 2023). We further combine β_i and MK tests to estimate the significance of the trend change. The MK test is sensitive to monotonic trends, meaning it detects whether the data consistently increases or decreases over time. It is robust against outliers and also does not rely on assumptions about the data distribution. The MK test considers statistical variables S for time series data ($x_1, x_2, \ldots, x_n$) (Chukwuka *et al.* 2023):

$$S = \sum_{i=1}^{n=1} \sum_{j=i+1}^{n} sgn(x_j - x_i) \tag{2}$$

When β_i is positive, it implies a positive trend, and when β_i is negative, the trend is negative. Because the original MK test is sensitive to serial auto-correlation typical of hydrological and meteorological time series, MMK tests are highly recommended. To ensure a high certainty of our results, we employed the original Mann–Kendall (Mann 1945; Kendall 1948) and MMK (Hamed & Ramachandra Rao 1998; Yue & Wang 2004). The MMK and Theil–Sen Slope estimator were employed using the pyMannKendall python package (Hussain & Mahmud 2019).

2.4. Change point detection of time series

Change point detection is important for monitoring changes in environmental patterns, crucial to understanding and mitigating environmental issues. In this study, we employed the Pettitt test for significant change point detection in daily surface water time series using the trend component. The Pettitt test is calculated as:

$$K_T = \max|U_{t,T}| \tag{3}$$

$$U_t = \sum_{i=1}^{t} \sum_{j=t+1}^{n} sgn(X_i - X_j) \tag{4}$$

For significant statistics, the change point in the series occurs at K_T (Parajuli *et al.* 2021). The Pettitt test (Pettitt 1979) was implemented in Python using the pyHomogeneity package (Hussain *et al.* 2023).

2.5. Correlation analysis and classification of deficit and excess years

Pearson's correlation analysis was employed to estimate how surface water responds to seasonal precipitation variation over the basin (Figure 1(b)). Mean monthly catchment precipitation and surface water area for each water body were correlated for six temporal lags at 0.05 and 0.01 significance levels.

We also calculated monthly and yearly rainfall anomalies for the entire active basin. The formula of Goswami *et al.* (2023) is used for the calculation and classification of excess and deficit years with respect to precipitation and percent deviation of the mean (climatology). A year is classified as an excess year when the percent deviation of the mean is >10%, and as a deficit year when it is less than −10%; otherwise, it is considered a normal year (Goswami *et al.* 2023). We further implemented the Köppen–Geiger (Köppen 1900) climatic zonation (Beck *et al.* 2023) for the period between 1991 and 2020 over LCB to spatially relate precipitation seasonality with surface water variations.

A common limitation of the methods and dataset lies in the use of gridded precipitation dataset instead of *in situ* data for analyzing rainfall events. However, the choice of ERA5 reanalysis is quite suitable for the study as this has proven high performance in detecting rain events over the Sahel and West Africa (Gbode *et al.* 2023; Saley & Salack 2023). Despite its strengths, ERA5 has also shown poor performance in some parts of West Africa (Quagraine *et al.* 2020; Goudiaby *et al.* 2024). Despite the robustness of GWP, we noted some underestimations of daily water extent in Lake Fitri partly linked to spectral reflectivity of clay dominated muddy water and the shallow water levels in some seasons. Also, between 2019 and 2021, we found possible underestimations (artifacts due to clouds and missing data) of Lake Iro by GWP.

3. RESULTS

3.1. Temporal and spatial surface water dynamics

3.1.1. Temporal and spatial surface water dynamics in Lake Chad

It is observed that Lake Chad water depicts marked seasonal patterns across the monitoring period (2003–2022). The maximum water area in all the pools is observed between December and January (Figure 2). In Lake Chad, the inter-seasonal surface water level varies between ~1,500 and ~3,800–4,000 km^2. Despite this, the Northern pool exhibits more sharp seasonal trends than the Southern pool. This also explains the presence of water in the Southern pool year-round, in contrast to the Northern pool which experiences significant seasonal fluctuations. The annual concentration of water in the Southern pool is partly explained by the huge contribution of streamflow from Chari-Logone Rivers which accounts for over 80% of discharge to Lake Chad. These are perennial rivers fed by several ephemeral streams of the tropical savanna zone of the basin.

On a daily basis, the Southern pool shows a high water area above 2,400 km^2 at the beginning and end of each year with the exception of drought years (2006–2017). For wet years (2004, 2018, 2019, 2020, 2021), surface water area between day 1 and around day 66, and between 301 and 365/366, ranges between 2,200 and about 2,400 km^2. With the exception of extremely dry years, the water area between 67–300 days of the year ranges from 1,600 to 2,000 km^2. In contrast, the Northern pool's maximum water area ranges between 1,600 and ~1,700 km^2 (Figures 2 and 3). With the exception of 2004, 2012, 2013, 2015, 2020, and 2021, the Northern pool only fluctuates between ≤200 and ~800 km^2 (Figures 2 and 3), which only stays for a few days of the year (Figures 3 and 4).

The wide remarkable difference between surface water extent in the Northern pool as opposed to the Southern pool could be explained by three aspects. First, the Northern pool is sourced by the Komadugu-Yobe River which has a low annual discharge linked to its long distance flow across the Sahelian and desertic part of the basin and increased dam construction upstream. This river system only contributes about ~2% of the total annual discharge to Lake Chad. Secondly, the Northern pool is exposed to hyper-arid climatic conditions with relatively high evaporation rates. Recent satellite images also show that the Northern pool is more encroached by desert sand than the Southern pool, which has resulted to some sort of infilling of

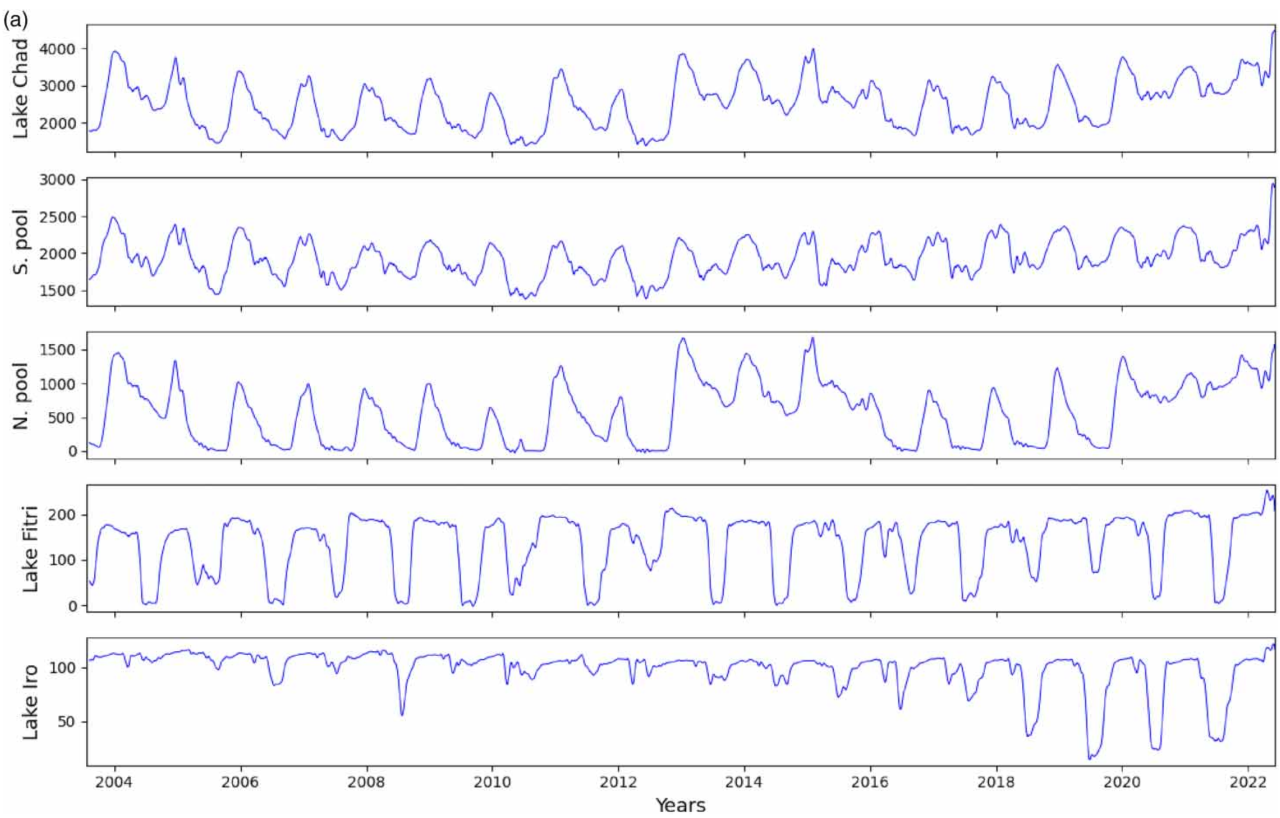

Figure 2 | Temporal dynamics of open water bodies area (in km^2) based on the GWP for (a) lakes and (b) reservoirs/dams. (*continued.*).

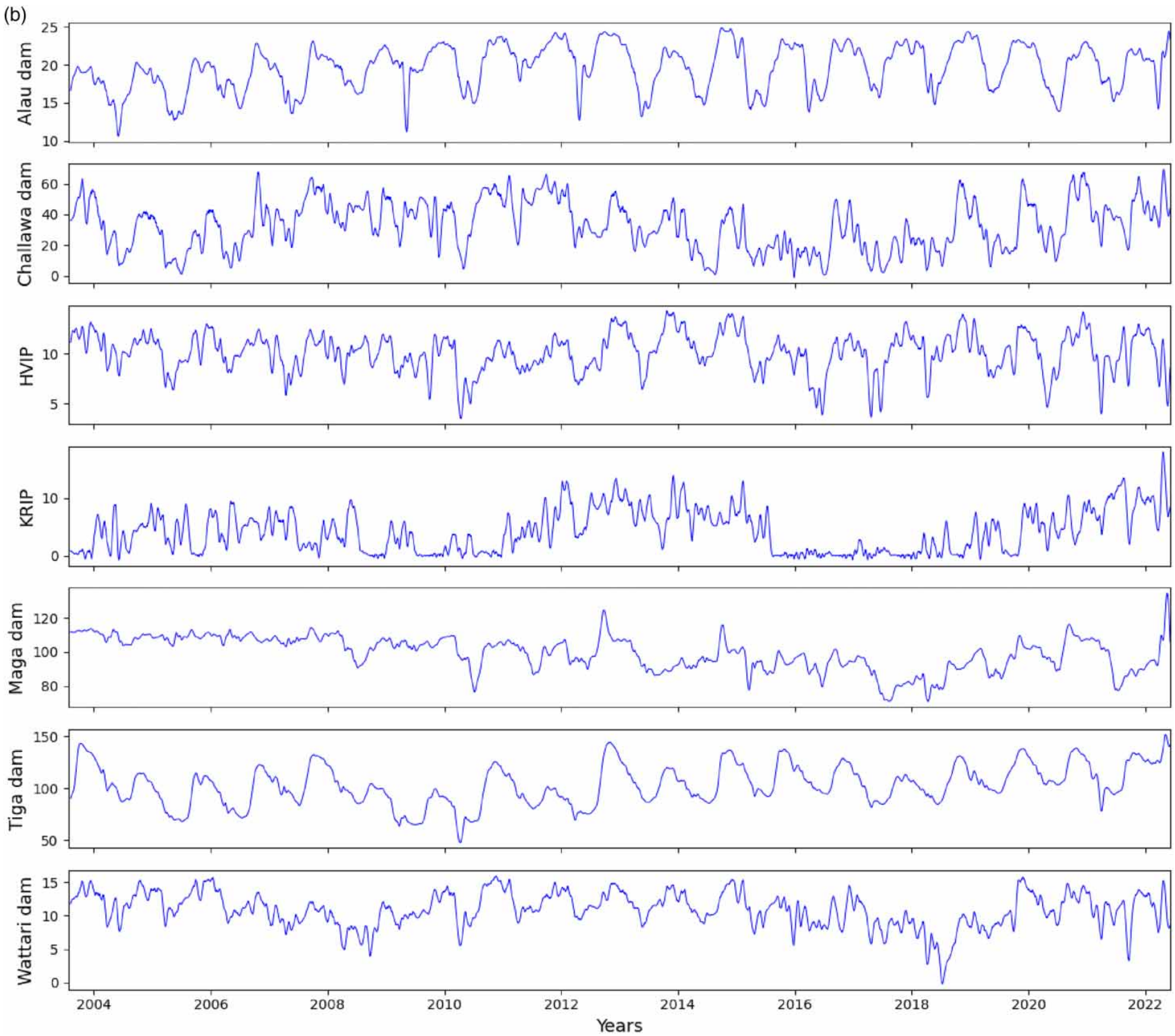

Figure 2 | Continued.

the pool (Supplementary material, Figure S2). Lastly, the development of the Great Barrier between the two pools has hindered the free circulation of water that formerly existed within the lake system. This barrier is only bridged when the Southern pool is flooded.

Figure 4 shows the highly variable nature of the Northern pool. For some years, e.g. 2012, the Northern pool only contains water for about the first 30 days of the year (i.e. in January), but in the last three years (2020, 2021 and 2022), the Northern pool is slowly recovering. It should be borne in mind that the water duration in the Northern pool is also highly controlled by surface water volume and areal extent of the Southern pool. Though the Northern pool is directly sourced by the Kamadugu-Yobe River system which contributes ∼2% surface flow into Lake Chad, as well as direct rainfall and groundwater, the Northern pool receives a significant amount of water via the Great Barrier following flooding of the Southern pool around December-January, especially in wet years. This partly explains why seasonal water (∼1–150 days) concentrates between the Great Barrier and the Northern pool (Figures 3 and 4). In the Southern pool, the shallow depths of the archipelagoes also harbour water that stays only for about half a year, though the recent years show almost a complete recovery of the Southern pool (Figures 3 and 4). In contrast to the Northern pool, the Southern pool is not subjected to continuous desert sand intrusion (Supplementary material, Figure S2).

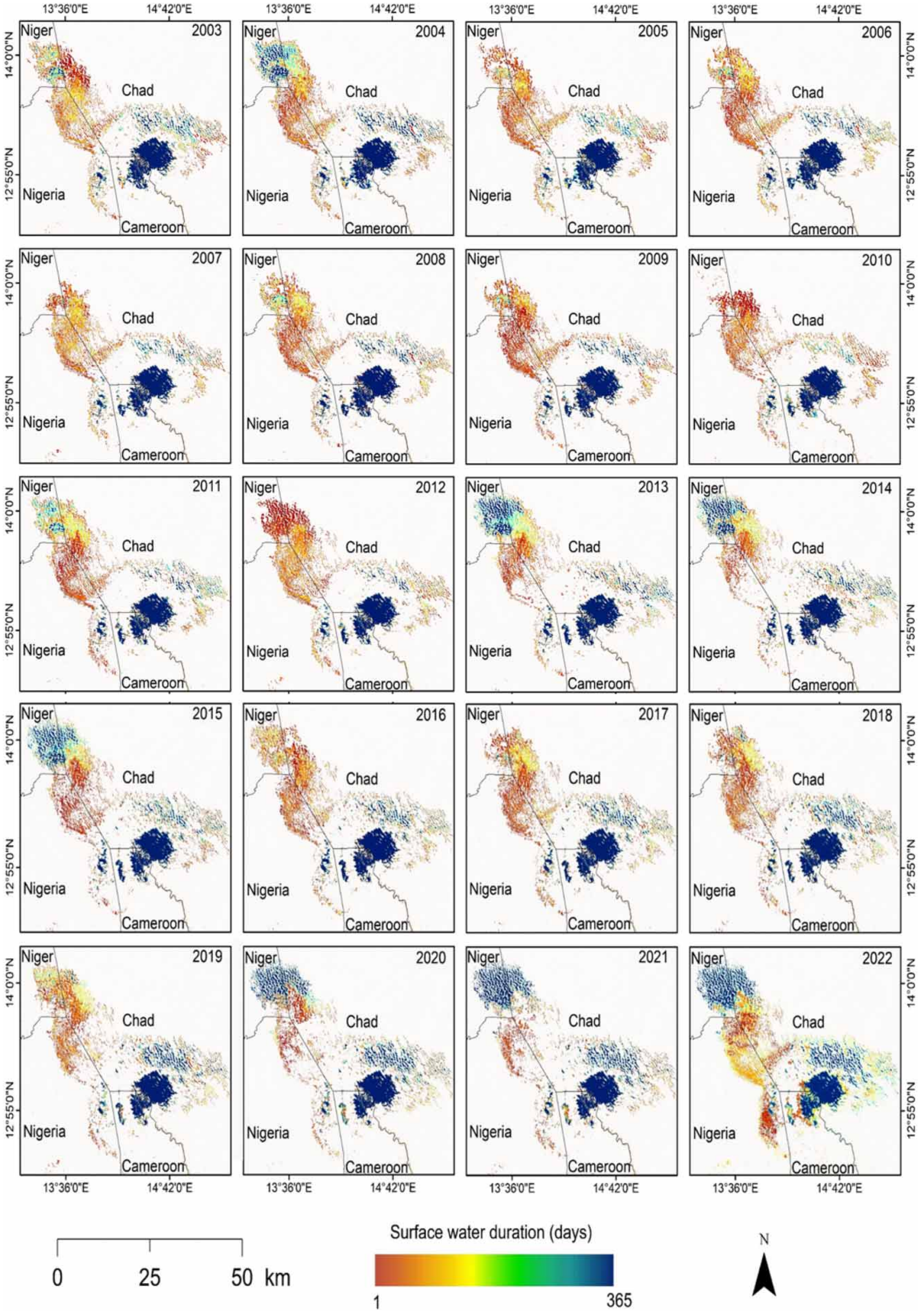

Figure 3 | Spatiotemporal surface water duration (DOY) per year in Lake Chad between 2003 and 2022 from GWP.

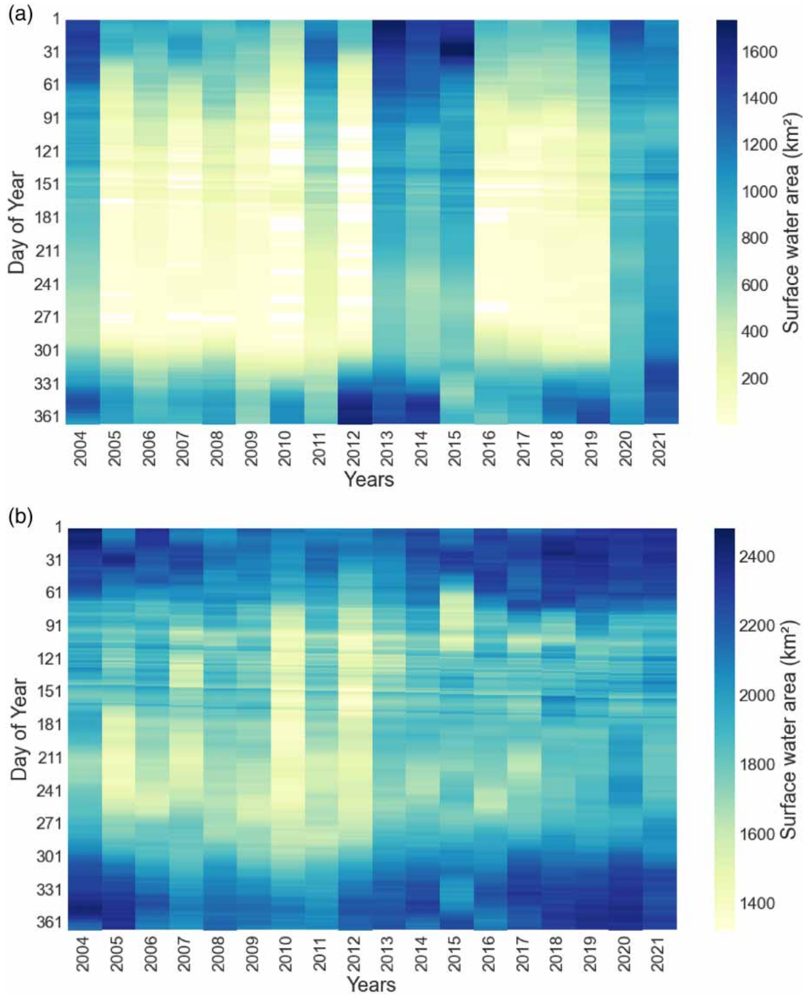

Figure 4 | Daily surface water extent in northern (a) and southern (b) pools of Lake Chad from GWP.

3.1.2. Temporal and spatial surface water dynamics in Lakes Fitri and Iro

Besides Lake Chad, other natural lakes (Lake Fitri, endorheic, and Lake Iro) are very vital in supporting ecosystems and life in the LCB. Lake Fitri is a miniature Lake Chad, a relic of the historic Mega Lake Chad located at the interface of Sahelian and hyper-arid climatic zones of the basin. The seasonal rivers, Bartha and Bahr Azoum, contribute water to Lake Fitri and Lake Iro, respectively. Similar to Lake Chad, Lake Fitri in the Sahelian part depicts marked seasonality as opposed to Lake Iro in the Sudano-humid zone (Figures 2, 5, 6), with highly contrasting spatiotemporal patterns (Figure 5).

In Lake Fitri, we observed that the maximum water area extent is reached between the 1st and 59th day and between the 305th and 365/6th day of the year (Figure 5).

Though these maxima are experienced, our analysis reveals that the areal coverage is quite negligible (Figure 5), as such Lake Fitri exists in a larger part of the year (~60–304 days) as a shallow water body. Surface water area between the 1st and ~150th day around the lake also corresponds to flood recession as a result of flash floods from river Bartha and early torrential rains in May–June in this Sahelian section of the basin. Thus, the maximum surface water area reached in the later days of the year (~305th–365/6th) partly reflects the time lag between precipitation, stream flow and lake water levels. With the exception of 2012, 2016, 2018, 2019, and 2022, fewer years in the monitoring period showed a duration of water that reached 365 or 366 days in Lake Fitri (Figure 6). This seasonal pattern in the cycle of Lake Fitri is also well explained by the seasonal nature of its source river (Bartha), as well as the seasonal progression of rainfall from the south to the northern arid zone of the basin. The extension of its contributing basin to hyper-arid areas also accounts for huge

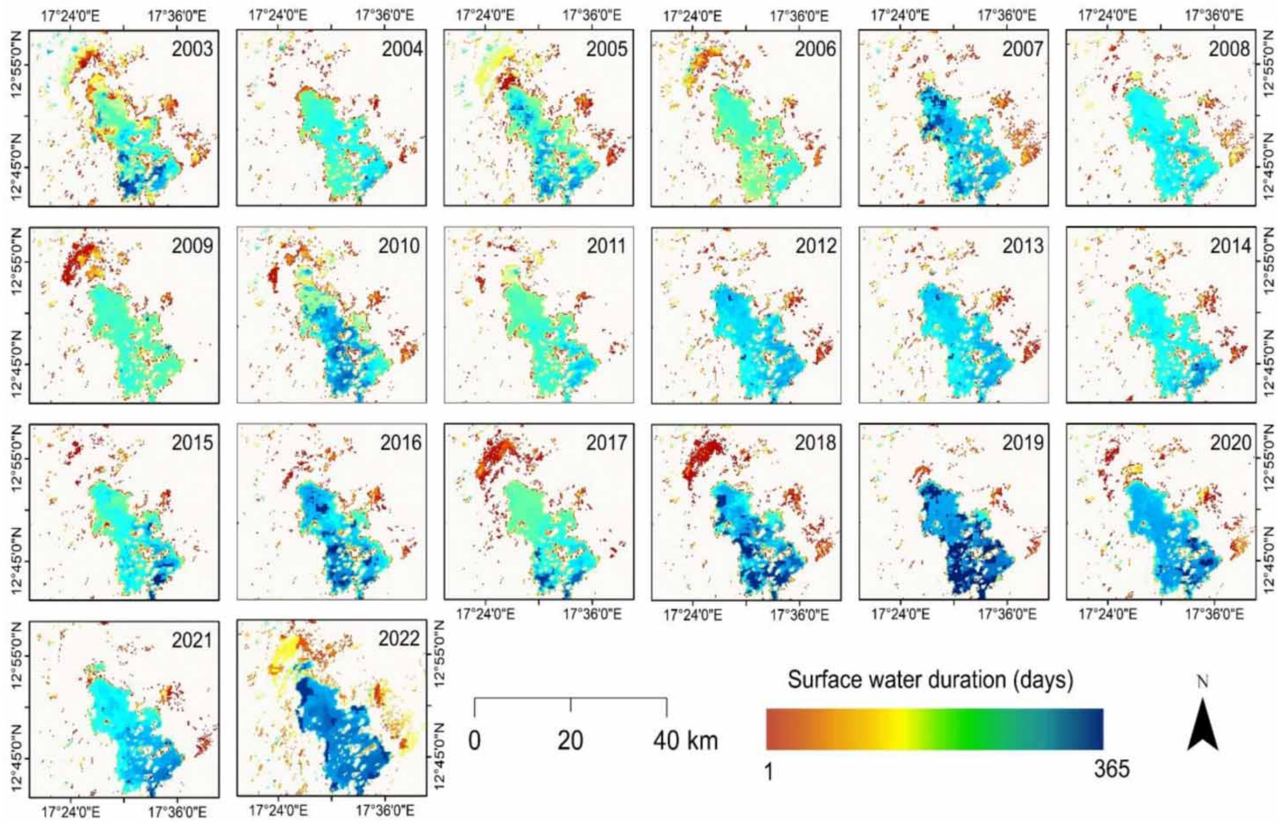

Figure 5 | Spatiotemporal surface water duration (DOY) per year in Lake Fitri between 2003 and 2022 from GWP.

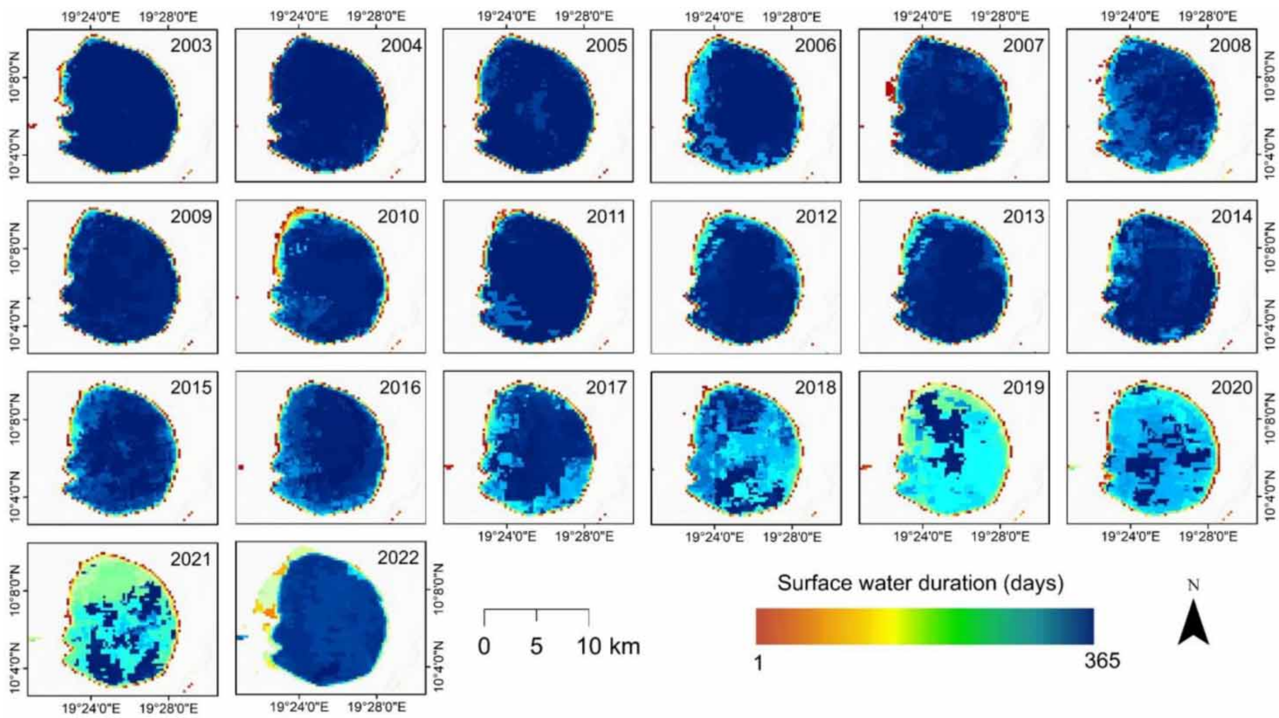

Figure 6 | Spatiotemporal surface water duration (DOY) per year in Lake Iro between 2003 and 2022 from GWP.

water loss via evaporation. However, we noted some underestimations of GWP over the surface water extent of this lake due to its shallowness and muddy nature in some seasons of the year. For example, between April and May, field reports reveal that the lake depth reduced to about less than 2 m and became increasingly muddy. This poses a problem to ambiguous spectral reflectance between clay soil and shallow water with high sediment content or shallowness that the reflectance of lake's ground is dominantly registered by the optical sensors used in GWP computations.

In contrast, seasonal patterns of Lake Iro (Figure 6) in the south sub-humid zone of the basin are less pronounced (between 2003 and 2016), with surface water lasting for 365/366 days/year. From 2017 to 2021, the lake illustrates very pronounced seasonal patterns, shrinking and reduction in surface water duration and areal coverage.

Between 2018 and 2021, much of the lake's water showed to only stay for less than half a year, ~170–290 days (Figures 2 and 6), but recovered in 2022.

3.1.3. Temporal and spatial surface water dynamics in reservoirs/dams

Reservoirs/dams respond to human controls of infilling and release of water for diverse uses. This explains their relatively high concentration of water across all seasons (Figure 2, 7 and 8), with the exception of drought-affected years or years with over-usage of water, e.g in KRIP between 2009 and 2011 and between 2016 and 2019 (Figure 2). The Tiga and Challawa dams are very vital for rice crop cultivation and seasonal crop cultivation in northern Nigeria. While the water area in Tiga Dam remains quasi-stable (Figure 7), Challawa Dam depicts extreme events of hydrological droughts, with a considerable shrinking of the dam size between 2004 and 2006, and between 2014 and 2020 (Figure 2). In the Challawa Dam, surface water stays only for about 1st to ~345th day of the year. An important portion of surface water in the Tiga Dam lasts for up to 365/366 days each year. The Wattari Dam, proximate to the Challawa Dam showed quite similar seasonal patterns (Figure 2). The Alau Dam and the HVIP are subject to seasonal climatic contrasts of stream discharge and rainfall patterns, aside from human controls of infilling and release (Figure 2). In Sahelian Northern Cameroon, the Maga Dam (Figure 8) serves the dying need of water for irrigation of rice and off-season (between December and February) crops (e.g. Sorghum or '*musgwari*' in Fufulde). The Maga Dam (Figure 8) is sourced from river Logone, an important tributary to Lake Chad.

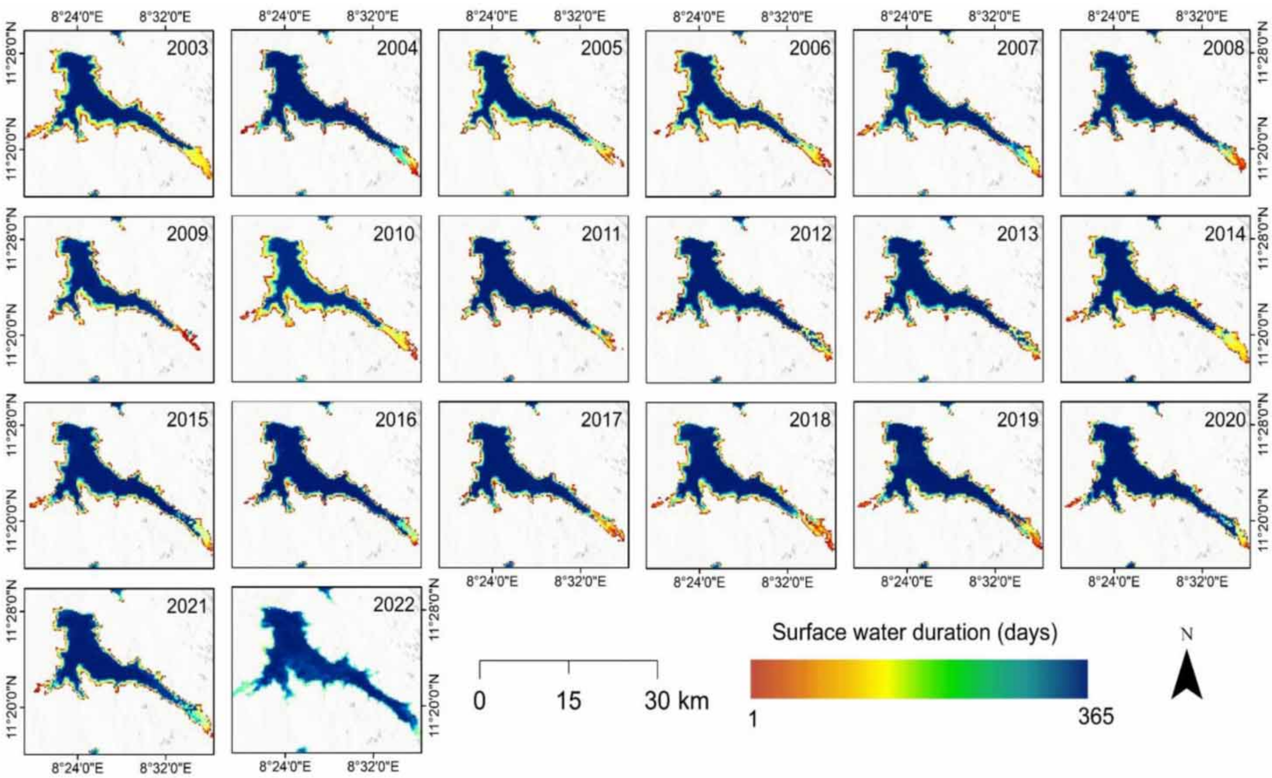

Figure 7 | Spatiotemporal surface water duration (DOY) per year in Tiga Dam between 2003 and 2022 from GWP.

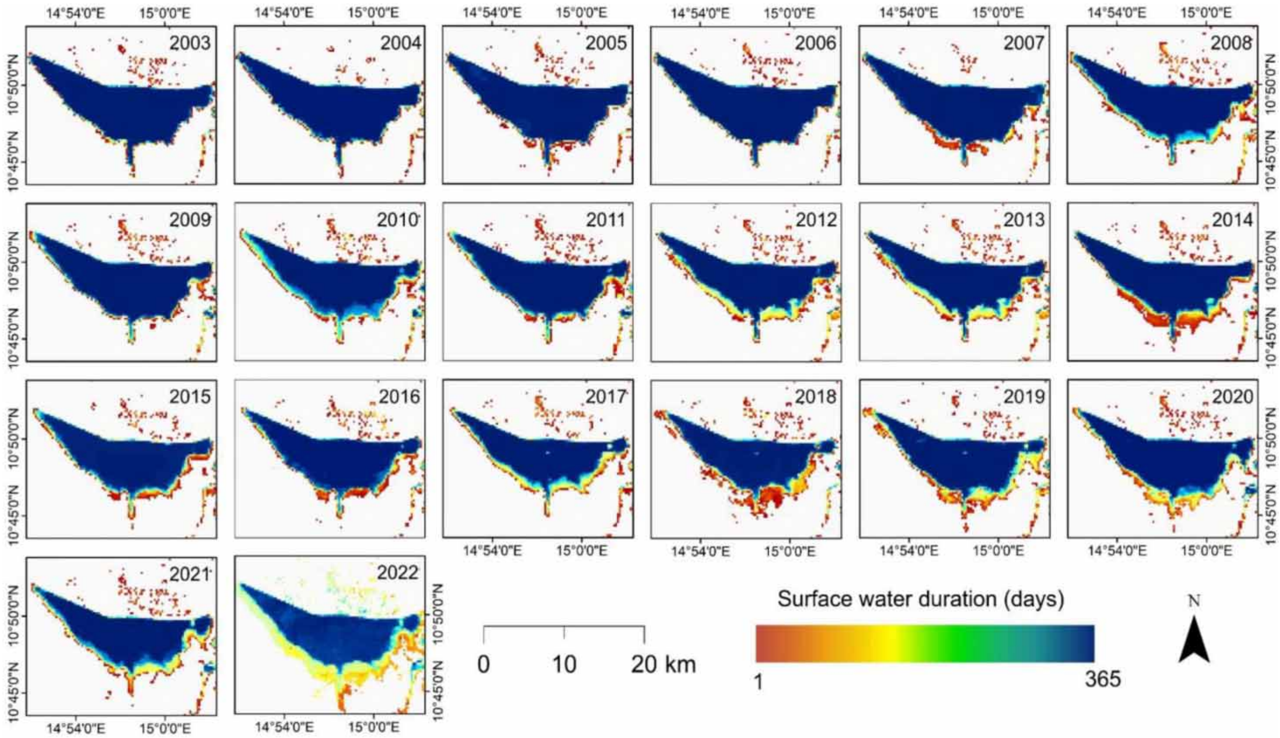

Figure 8 | Spatiotemporal surface water duration (DOY) per year in Maga Dam between 2003 and 2022 from GWP.

The latter showed a quasi-stable water area coverage from 2003 to 2010, then inter-seasonal and inter-annual fluctuations from 2010 to 2022, with a marked declining area coverage between 2013 and 2019 (Figures 2 and 8).

3.2. Seasonal patterns of surface water dynamics and trends

3.2.1. Seasonal and inter-annual variations in surface water bodies

Across the LCB, surface water in natural lakes exhibits pronounced seasonal contrast as opposed to reservoirs/dams. Maximum areal coverage in surface water in the lakes Chad, Fitri and Iro are reached at the beginning (January–Febuary) and end (November–December) of each year (Figure 9). Between the Northern and Southern pools of Lake Chad, a marked contrast exists (see Figures 3 and 4). While surface water area coverage is quasi-stable across all seasons in the Southern pool, the Northern pool only has minimal water coverage from April to October yearly. In Lake Fitri, the months of June, July, and August contain minimal surface water area.

Lake Chad only starts regaining its actual size after the lag time between precipitation and effective stream discharge from September through December (either from 245 to 365/366 days). Under semi-humid conditions, Lake Iro does not reflect marked seasonal fluctuations, though between July and August, the areal coverage of surface water is low (Figure 9).

Reservoirs/dams are characterized by human controls of infilling and withdrawals. No strict and unique seasonal pattern is explained by reservoirs/dams in the basin, despite that they respond to contrast in climatic zones, rainfall patterns, and seasonal stream discharge amongst others. Figure 10 shows three reservoirs/dams selected across different climatic zones of the basin.

Despite the location of the reserviors/dams in the basin, they all show an increasing water area around 180 days (around July) each year. This period corresponds to the onset of the wet season. They also each contain high water levels until the last quarter of the year, corresponding to the dry season. Here, water is used for off-season irrigation (Figure 1(a)). Though the Tiga Dam is located in a sub-humid zone with relatively high rainfall as opposed to the Alau and Maga dams in the Sahelian zones, they all illustrate similar seasonal patterns (Figure 10).

Inter-annual variations are also registered within the investigated period. Mean annual water coverage in Lake Chad varied from 2,952.85 to 3,114.43 km^2 between 2004 and 2021, respectively (Supplementary material, Table S1). Meanwhile,

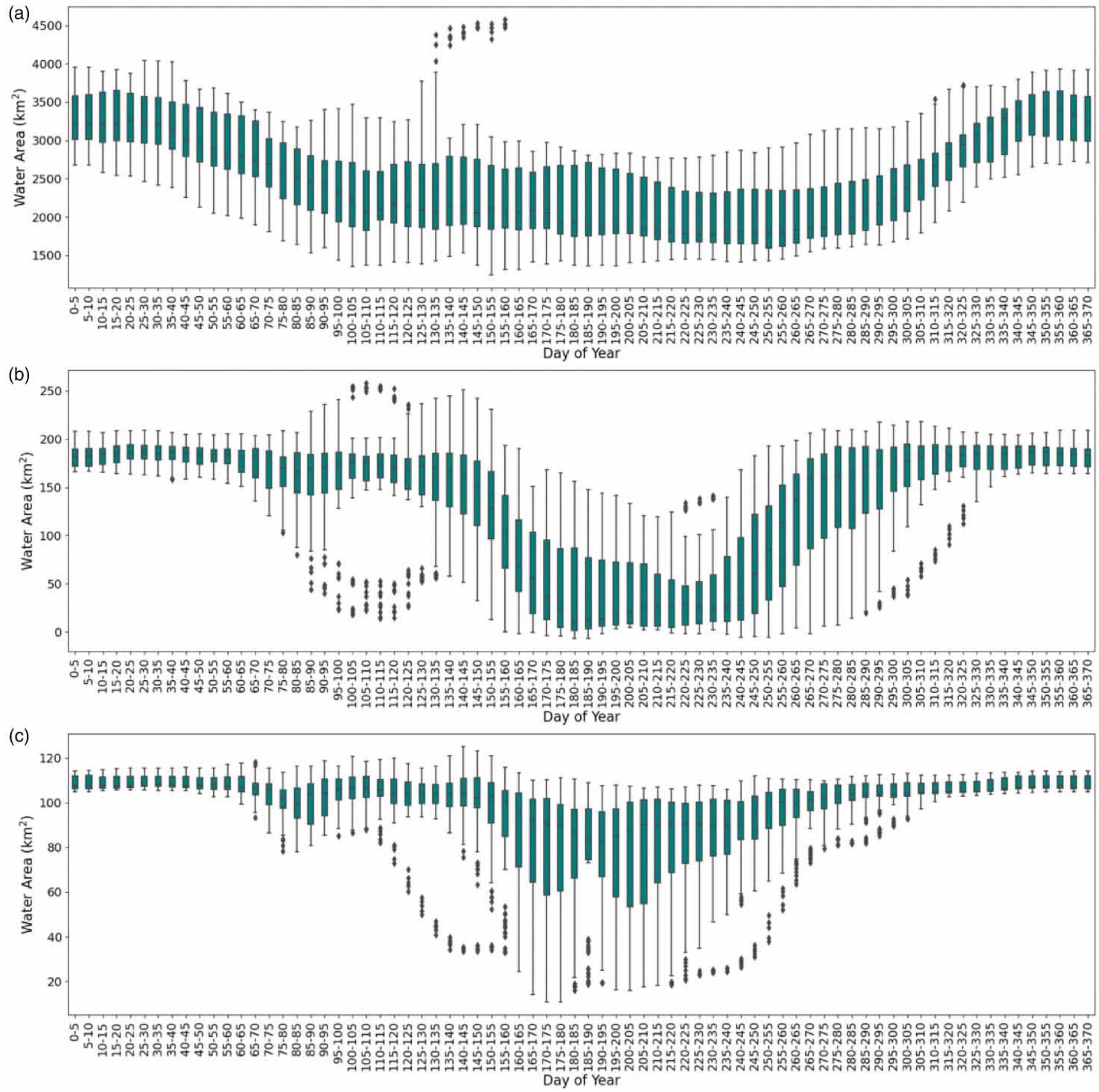

Figure 9 | Boxplots showing the seasonal variation in surface water area over the investigated time period for five daily intervals in (a) Lake Chad, (b) Lake Fitri, and (c) Lake Iro from GWP.

between 2005 and 2012 and between 2016 and 2019, the surface water area is below 2,500 km^2. This corresponds to dry years as opposed to 2004, 2013, 2014, 2015, 2020, and 2021 which are correspondingly wetter, with mean annual surface water coverage above 2,800 km^2 (Supplementary material, Table S1). However, this inter-annual trend is not identified in all Lake Chad pools. In the Southern pool, the mean annual surface water area varied from 2,030.44 km^2 in 2004 to 2,051.49 km^2 in 2021. Between 2005 and 2017, with the exception of 2010 and 2012, the Southern pool is limited at $\leq$1970 km^2, while in 2010 and 2012, the pool is between 1,600 and 1,723 km^2 (Table S1). The Northern pool demonstrates recovery and dwindling phases. Between 2005 and 2012 and between 2016 and 2019, the Northern pool does not contain water above 600 km^2, with just $\leq$350 km^2 of surface water area for most of the year (Figure 3 and Supplementary material, Table S1). However, it recovered in 2004, 2013, 2014, 2015, 2020, and 2021, though mean annual water coverage is not above

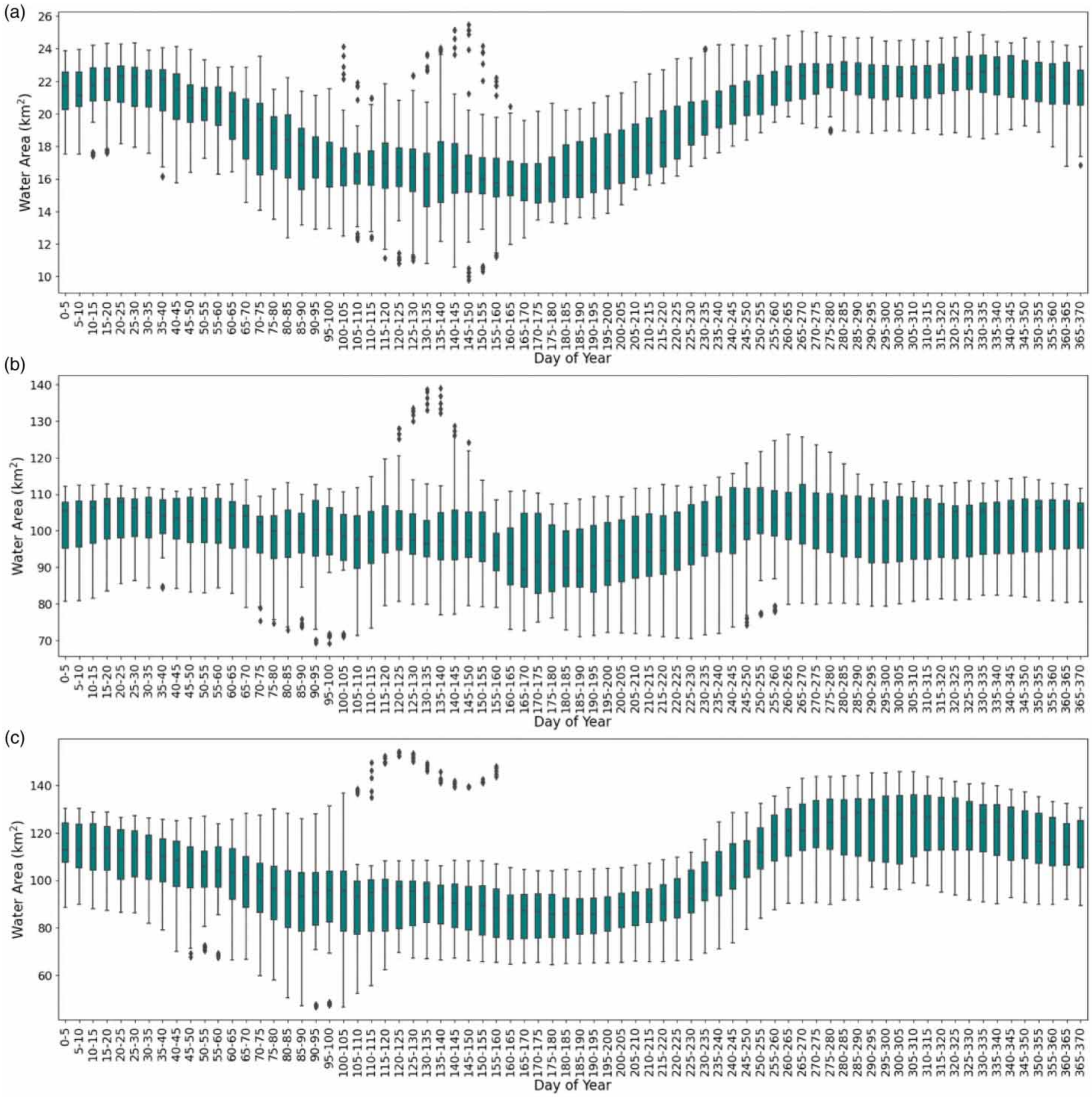

Figure 10 | Boxplots showing the seasonal variation in surface water area over the investigated time period for five daily intervals in (a) Alau Dam, (b) Maga Dam, and (c) Tiga Dam from GWP.

1,060 km^2. This period of recovery also corresponds to the same period in which Lake Chad recovers from dry periods as rainfall increases in the Sahel.

3.2.2. Seasonal and annual trends in surface water dynamics

Our results revealed that seasonal surface water is increasing in Lake Chad in all seasons (Supplementary material, Table S2) and annually (Table 1), either 0.0782 km^2/daily or 28.54 km^2/year. However, the trend analysis shows an increasing trend for Lake Chad, with exceptions for some seasons, i.e. January and February for the Northern pool and April for the Southern pool, where surface water showed no significant trends (Supplementary material, Table S2). However, both pools are increasing almost at similar trends (Table 1). Similarly, with the exception of July and September, all seasons showed significant

Table 1 | Estimated trends and change magnitude of open water bodies

Water bodies	tau	p*	s
Lake chad	0.157	**0.012**	0.0782
Southern pool	0.158	**0.000**	0.031
Northern pool	0.132	**0.003**	0.036
Lake Fitri	0.141	**0.000**	0.003
Lake Iro	-0.355	**0.000**	-0.0021
Maga dam	-0.439	**0.000**	-0.0032
Alau dam	0.175	**0.017**	0.175
Tiga dam	0.222	**0.000**	0.0034
Challawa dam	-0.042	0.457	-0.000
Wattari dam	-0.110	**0.008**	-0.000
KRIP	0.0125	0.807	3.341
HVIP	0.035	0.108	5.572

[a]In bold, significant at 0.05 level, light blue (increasing trend), and light orange (decreasing trend).

increasing trends in surface water area in Lake Fitri over the study time scale. Meanwhile, the annual increase rate is 1.095 km^2/year. In contrast, Lake Iro shows a declining trend (0.7665 km^2/year) across seasons and years (Table 1). The slight recovery of these Sahelian lakes is also partly explained by the recent increase in rainfall reported across the Sahel.

For reservoirs/dams, the trend is less clear than in natural lakes (Supplementary material, Table S2 and Table 1). Surface water duration in Maga Dam shows a continuous decline across all seasons and years, with an annual decrease rate of -1.168 km^2/year. This is going to have far-reaching implications on irrigated rice and off-season crop cultivation in the dry northern regions of Cameroon. The causes for such decline are unclear. In this same vein, the Challawa and Wattari dams in Northern Nigeria also showed a declining trend, though most of the seasons do not show any significant change trends in their surface water extent, but the annual rate of decrease is quite minimal (Table 1). The Tiga Dam showed significant increasing trends with seasons and years. Alau Dam also demonstrated seasonal and annual increase trends, but the rate of increase is quite minimal (Table 1). Though the Challawa Dam, KRIP and HVIP upstream of Lake Chad do not show significant seasonal trends, some seasons in Challawa Dam and HVIP showed quite significantly increasing trends in surface water duration and extent (Supplementary material, Table S2). In HVIP, surface water duration in August, October, and November showed significant increasing trends (Supplementary material, Table S2). The same scenario is observed in Challawa Dam for November, and KRIP in December (Supplementary material, Table S2).

3.3. Change points and shifts in surface water extent

Significant change points were identified in the monitored period (Figure 11).

Within the cycle of Lake Chad, a decreasing trend is observed between 2003 and 2012, with an average surface water area extent of 2,274.82 km^2. From 2012 to 2022, an increasing trend is noticed with an average surface water extent of 2,744.91 km^2. A significant change point in the time series is observed on 2012-10-14.

In the Southern pool, the change point is observed in 2013-10-16 with a shift in the surface water area from 1,858.22 to 2,028.40 km^2 after the change point. In contrast, in the Northern pool, the change point occurred on 2012-08-14. Here, the surface water area shifted from 408.04 to 721.61 km^2 after the change point. In Lake Fitri, a decreasing trend is observed during 2003–2012, with the average surface water area being 123.84 km^2. From 2012-03-20, a significant change point is observed until 2022 with an increasing trend and average surface water extent of 144.35 km^2. In comparison, Lake Iro depicts a decreasing trend throughout the investigated period. It significantly shifted from 105.56 km^2 between 2003 and 2013 to 91.48 km^2 between 2013 and 2022. In Lake Iro, a significant change point with an increasingly declining shift was registered on 2013-02-27 (Figure 11). In reservoirs/dams, significant change points were also observed.

3.4. Open surface water dynamics and its response to rainfall in LCB

Surface water areas extent respond to rainfall seasonality. We found that rainfall at the catchment scale and surface water extent show a strong and significant correlation for some of the investigated water bodies (Figure 12).

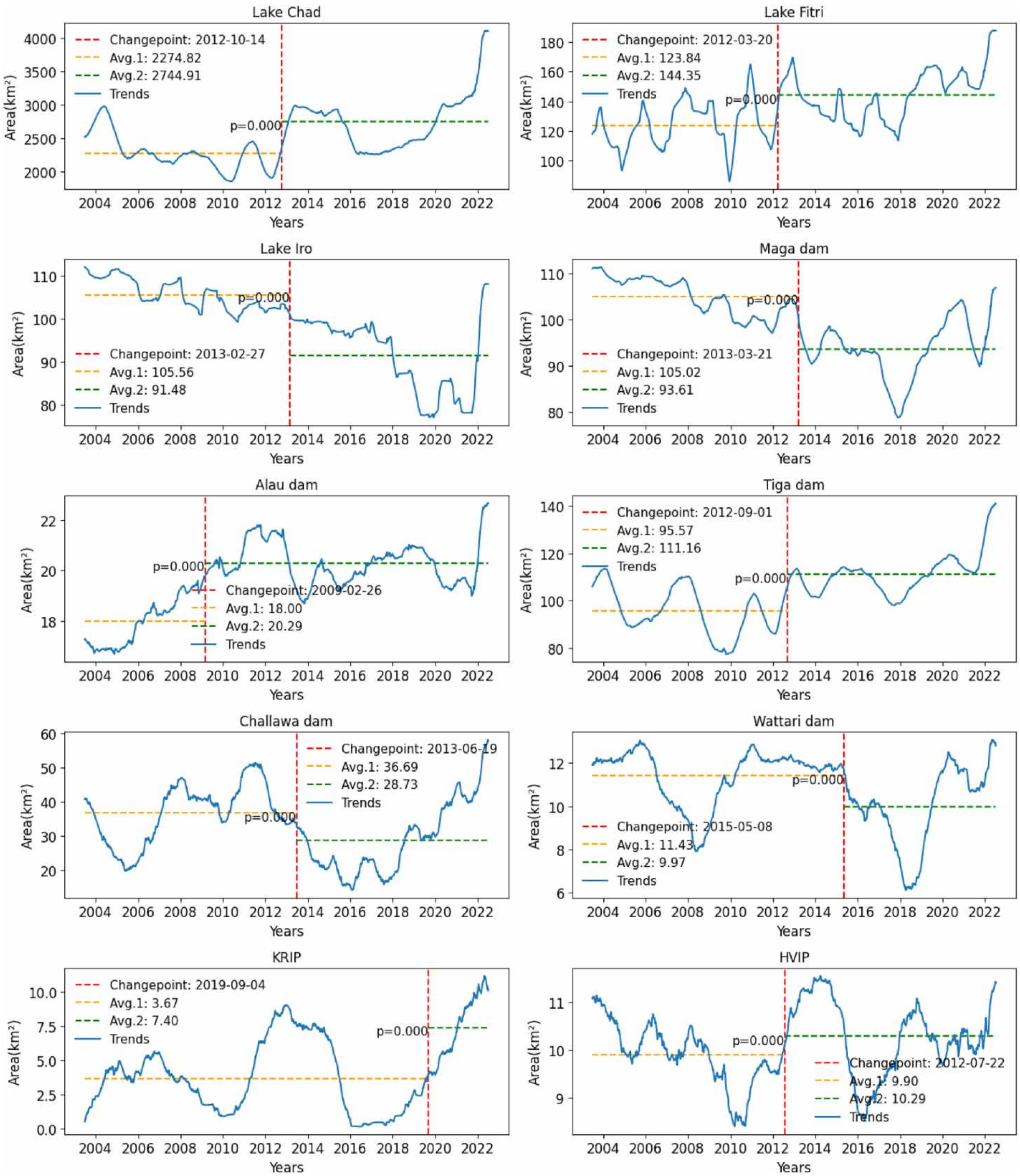

Figure 11 | Change points and shifts in surface water extent in open water bodies.

In the case of Lake Chad, the maximum surface water extent shows a 4- to 5-month lag to regional precipitation (Figures 12 and 13). Here, the correlation is found to be strongest at the fifth temporal lag ($r = 0.70$, $p = 0.000$) (Supplementary material, Figure S1). This positive relationship starts becoming important after three months of lag time (Figure 13). This relationship explains the time lag between rainfall and stream discharge in the basin and the corresponding increase in surface water in

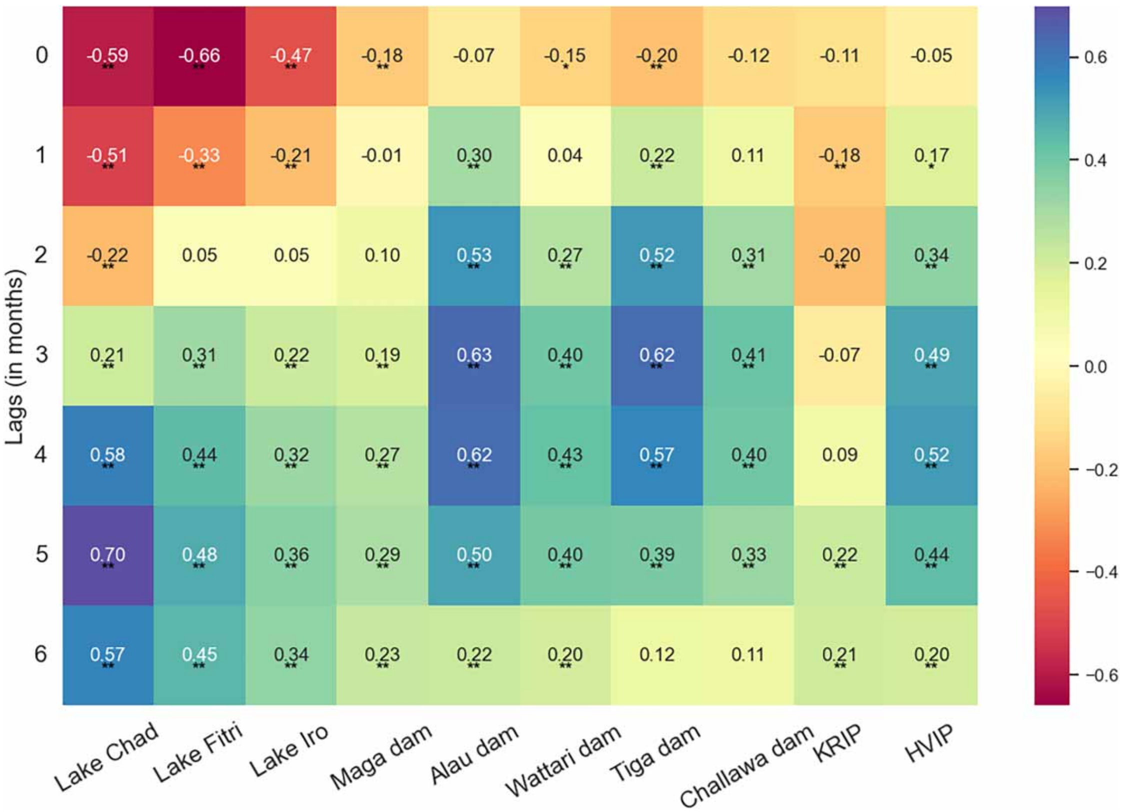

Figure 12 | Temporal lag correlation between catchment monthly rainfall and surface water extent in open water bodies.

open water bodies in the downstream area. In this regard, the maximum surface water extent in Lake Chad is reached between December and January each year (Figures 3, 4 and 9). Also, the long time lag in rainfall and maximum surface water extent of Lake Chad is linked to the extensive and climatically diverse nature of the basin, wherein much of the precipitation is being lost via evapotranspiration which is high in the Sahelian and desert margins of the LCB (Figure 13).

Other lakes of natural origin showed significant but less than 50% correlation at the 4th lag. This is partly explained by the influence of desertic and Sahelian climatic conditions of high temperatures and evaporation which results in a loss of surface water from precipitation in rivers before it arrives in the lakes (Figure 13). Both rivers Bartha and Bahr Azoum (Figure 13) which feed the lakes Fitri and Iro, respectively, are subject to great seasonal contrast. Lake Fitri is highly exposed to hyper-arid conditions, thus explaining its marked seasonality (Figures 5 and 13).

On the contrary, reservoirs/dams showed strong and significant correlations at lags two and three. This implies that precipitation could contribute to the maximum surface water area in most reservoirs/dams in LCB with a temporal lag of 2–3 months (Figure 13).

Reservoirs/dams respond differently to rainfall seasonality in the basin as also demonstrated in Figures 12 and 13 irrespective of their location in the LCB. However, some reservoirs/dams (Maga Dam and KRIP) illustrate significant but below 40% of correlation with the second to the fifth lags. This contrast could be attributed to other drivers of surface water area than precipitation. Also, Maga Dam as well as Lake Iro showed a declining trend in recent years (Table 1 and Supplementary material, Table S1, Figure 14), attributed to factors not accounted for here.

Open surface water variation and anomalies also align with periods of climatic extremes in LCB. Figure 14 reveals that years of excess and deficit correspond closely to similar signals of monthly surface water extent and duration following the corresponding lag time. Across the monitored period, four periods of wet and three periods of dry conditions were identified (Figure 14). Following the identified time lag between rainfall and surface water extent in open water bodies, the impact of wet and dry years is quite visible across the lakes in the LCB (Figure 13).

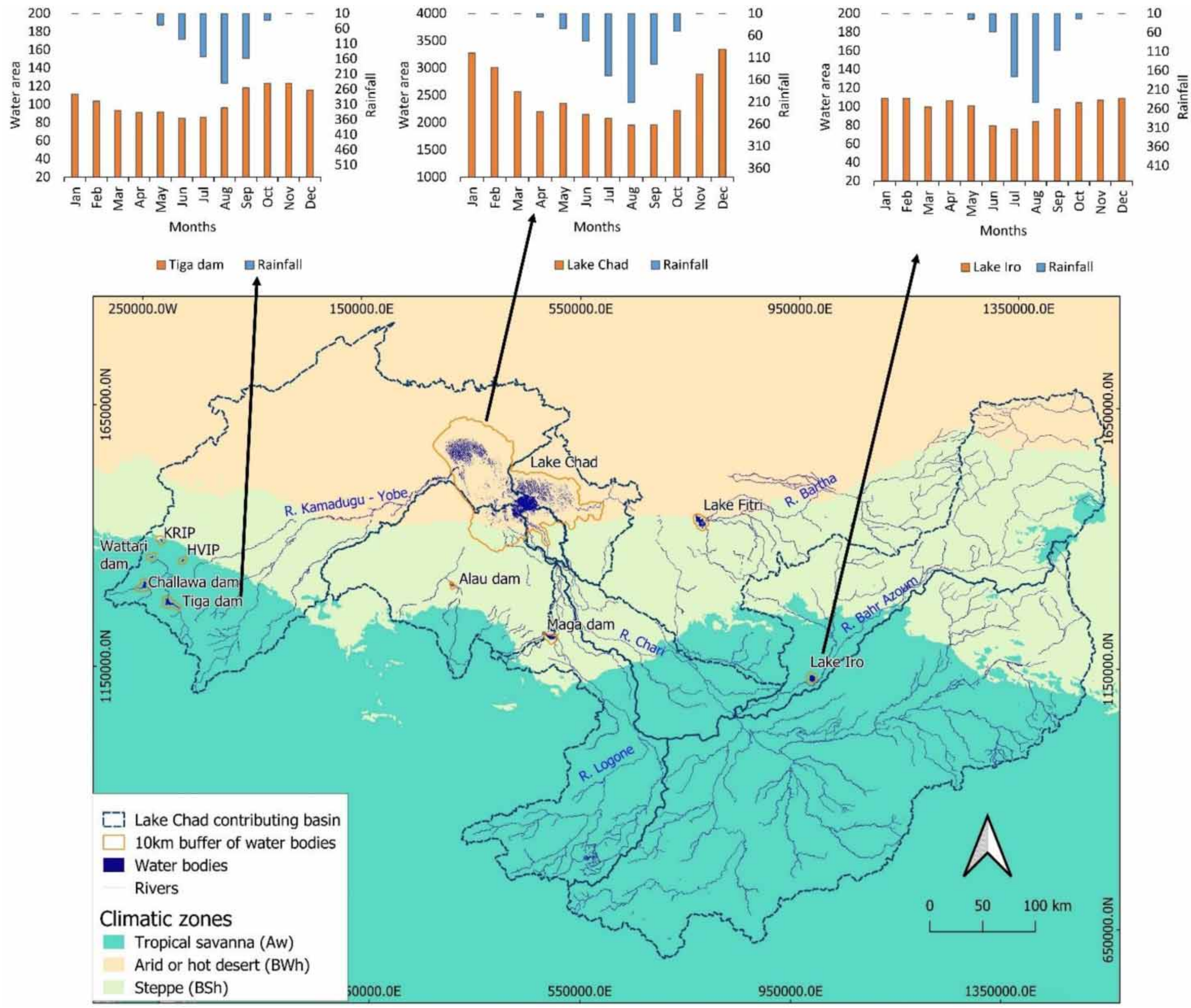

Figure 13 | Köppen -Geiger climatic zones (Beck *et al*. 2023), mean monthly rainfall at basin scale (mm), and surface water area (km^2) for selected open water bodies in LCB.

However, in every case, reservoirs/dams irrespective of their climatic location (Figure 13) do not portray the same signals as natural lakes (Figure 14). For example, the excess or wet year of 2005 is not reflected in the Alau and Tiga dams. Likewise, the deficit years of 2009 and 2014 are not reflected in the Alau and Maga dams, and the Tiga, Alau and Maga dams, respectively (Figure 14). It is also important to note that the droughts or rainfall deficits observed in 2021 did not affect Lake Chad, Lake Fitri, and the Tiga Dam. This may be partly explained by the role of groundwater concentration on the water balance of Sahelian lakes as well as less human influence within that year. Though Tiga Dam recovered, this anomaly is not as strong as in the wet years. Thus, this might be explained by the combined influence of human controls on dam water dynamics and the relatively wetter climatic location of the dam (Figure 13).

4. DISCUSSION

4.1. Seasonal extent and dynamics of open surface water bodies

The Lake Chad, Lake Fitri, and Lake Iro are characterized by different seasonal cycles reaching their maximum extents in December and January. This has been reported in previous studies. To this inter-annual variability, we must add a strong seasonality, characterized by lake flooding which occurs between December and January (Southern pool) and between February

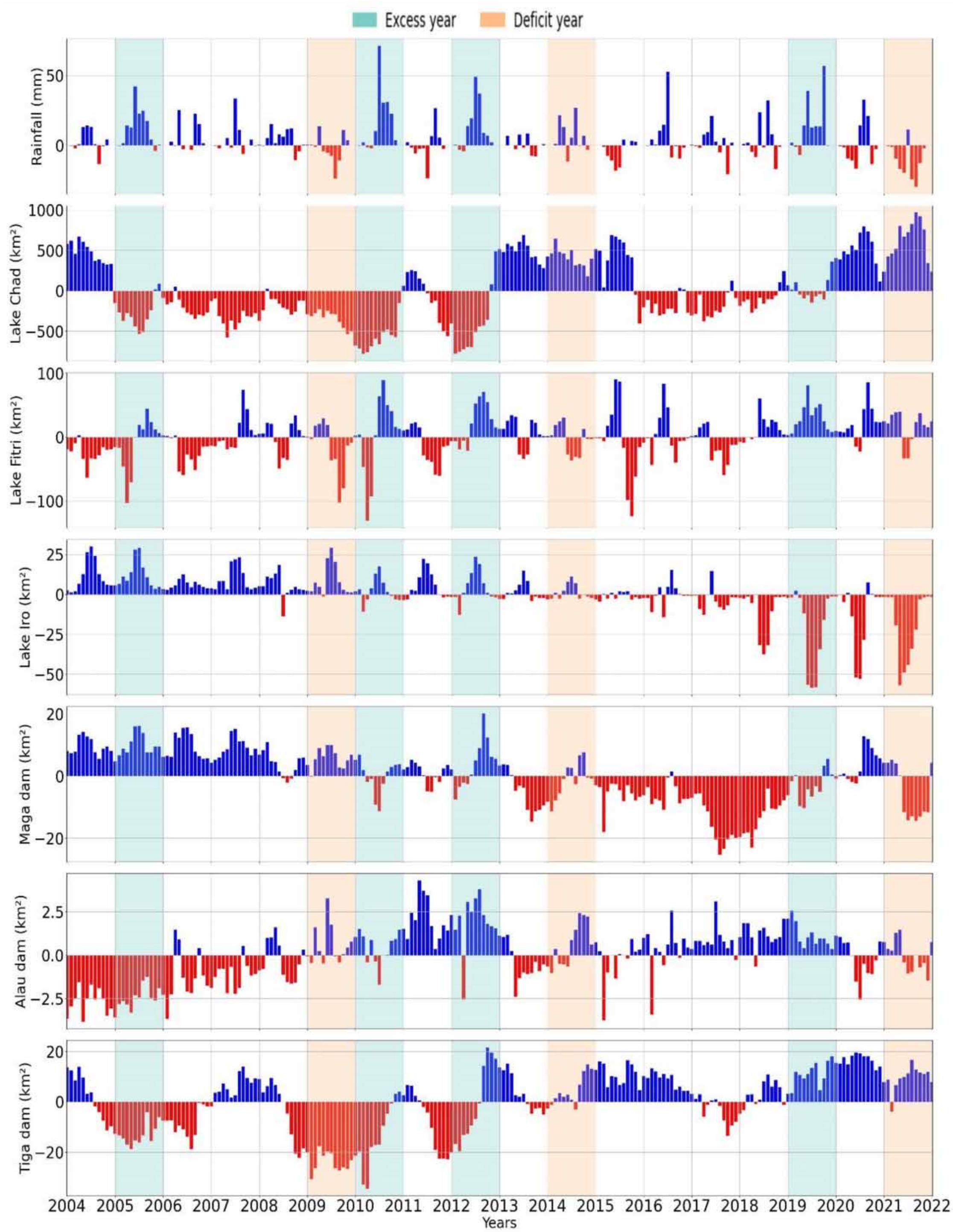

Figure 14 | Monthly rainfall and surface water extent anomalies across excess and deficit years.

and March (Northern pool) and by low water in August (Magrin *et al.* 2015). The daily and seasonal dynamics observed in Lake Chad's cycle are also explained by the variability of rainfall and streamflow into the lake system. The Chari River contributes 95% of the surface flow to Lake Chad and explains much of its seasonal cycle. Magrin *et al.* (2015) reported that the Chari River regime is a tropical type with an annual flood marked by a peak toward the beginning of November and a pronounced low flow in March–April. This is also reflected in the annual cycle of Lake Chad, with high waters observed from November to February (Figures 3, 4, and 9).

River Kamadugu-Yobe, a second contributor to Lake Chad's waters was estimated to have brought approximately 0.5 km^2 of water per year to the lake for the period 1990–2000, i.e. 1.8% of Chari's contributions (Magrin *et al.* 2015). The construction of two dams (Tiga in 1974 and Challawa in 1992) upstream of the Yobe River resulted in a modification of the flow to Lake Chad. Magrin *et al.* (2015) recently reported that the reduced flooding of the Hadejia-Nguru floodplain, which leads to less water loss through evaporation, partially compensates for the water withdrawals from the dams. The El-Beïd River contributes to the rest of Lake Chad's surface flows. Its streamflow reaches its maximum between November and December (Bdliya & Bloxom 2007.; Magrin *et al.* 2015), but the flow rates vary from one year to the next depending on the Logone floods (Magrin *et al.* 2015). The highest water levels observed in Lake Chad between December and January (Figures 3, 4, and 9) is a combined response of the lag time resulting from the discharge of the aforementioned river systems.

Inter-annual surface water extent also varied considerably across the basin. We observed that the mean annual water area for Lake Chad between 2004 and 2021 stood at 2,475.64 km^2. However, significant differences exist between area estimates of water extent from various optical sensors. In comparison with Landsat-derived water extent datasets, we found a difference in annual area estimates ranging from $\leq$249 to $\geq$901.6 km^2 (Supplementary material, Figure S5) between the JRC water product and MODIS-based GWP of this study. Nonetheless, similar spatiotemporal seasonal patterns of surface water variations are observed by both optical sensors Supplementary material, Figures S3 and S4. More so, during the drought years of 2005–2012 and 2016–2019, both products effectively estimated lower water coverage over the lake, both below 2,500 km^2 (Supplementary material, Figure S5) as observed in this study. Despite this, some Landsat-based studies (e.g. Ekpetere *et al.* 2023) rather underestimate surface water extent in Lake Chad as compared to Pekel *et al.* (2016), Buma *et al.* (2018) and Pickens *et al.* (2020). It should also be noted that surface water extent derived from Landsat sensors over the LCB was flawed during the period between 31 May 2003 and 2012 following the failure of Landsat 7 Scan Line Corrector (SLC). This resulted in a significant loss of valid pixels leading to huge data gaps and, thus, affecting the estimated water area extent during these periods. The aforementioned gaps are well observed over some Landsat surface water products (e.g. Pekel *et al.* 2016; Pickens *et al.* 2020) over LCB. Also, Herndon *et al.* (2020) observed that the JRC surface water dataset (Pekel *et al.* 2016) greatly underestimated the surface water extent in the Nigerian Sahel landscape. Mindful of sensor differences in surface water extent area estimates, our study revealed an increasing trend in Lake Chad water extent, which is in line with a previous study (Buma *et al.* 2018) that used Landsat for seasonal and annual surface water area extent estimates. Though surface water area extent may vary when estimated from both optical sensors, we found that seasonal and annual surface water extent in Lake Chad aligns with Global Landsat-based products (Pekel *et al.* 2016; Pickens *et al.* 2020) (Supplementary material, Figures S3 and S4). When compared with global Landsat-based surface water extent datasets of Pekel *et al.* (2016) and Pickens *et al.* (2020), MODIS-based surface water extent estimation is shown to be more robust to capture intermittent surface water, though smaller waterbodies may be underestimated due to the coarse resolution of the sensor (Liu *et al.* 2022). We also found more or less similar estimates of open water areas in Lake Fitri with findings by Talikun *et al.* (2019) using Landsat.

Similarly, our findings revealed interesting daily and seasonal dynamics of surface water extent in Lakes Fitri and Iro. As commonplace with optical sensors, we, however, noted some underestimations of GWP over Lake Fitri as compared with ground realities. This is partly linked to its shallow depth (at times < 2 m) and concentration of muddy water in some parts of the year. This poses a serious challenge to spectral reflectance registered by channels of optical sensors. Such underestimations from optical sensors were common between May and July (days 121–212), as observed also by Talikun *et al.* (2019). Also, possible artifacts were detected over Lake Iro between 2019 and 2021, though we observed similar patterns within the aforementioned period by other optical sensors products, e.g. the Landsat surface water product by Pickens *et al.* (2020). Consequently, our estimated trends and temporal correlations for these lakes may be flawed, but not incorrect as Talikun *et al.* (2019) also found that Lake Fitri doubled in size between 1972 and 2015.

4.2. Reservoirs/dams water dynamics and implications on LCB hydrological balance

Surface water in reservoirs depicted increasing trends extending beyond the season as opposed to lakes in the basin. Their seasonal pattern was explained more by human manipulation of infilling and water withdrawals (Figures 10, 12 and 14). It is largely reported that upstream dam construction has profound effects on downstream river systems and flow modifications. The Tiga and Challawa dams each control 80% of the flows into the Hadejia-Nguru wetlands (Thomas 2008) of the Kamadugu-Yobe Basin. The average annual flow in the upstream part of the Hadejia River has been reduced by 33%

after the completion of the Tiga Dam (1979–1989) (Chiroma *et al.* 2005; Sanni 2018). In the Chari-Logone Basin, Zilefac (2010) reported a 70% reduction of water supply by the Maga Dam to the floodplain from the Mandara Mountains. Between 1960 and 2000, Olowoyeye & Kanwar (2023) reported that the reduction in surface water of Lake Chad was entirely linked to climate change, population pressure, and water abstraction for irrigation.

Besides flood control, the Tiga Dam stores water for the KRIP, and the HVIP, while the Challawa Dam provides water for domestic use in Kano and supplement water deliveries for the HVIP. In Borno State of Nigeria, the Alau Dam was constructed between 1986 and 1989 to supply domestic and industrial water to Maiduguri town. Since the completion of the Alau Dam, the natural inflow of the Ngadda River (see Figure 1(a)) into Jere Bowl no longer takes place (Babagana *et al.* 2015), thus reducing the usual inflow to Lake Chad.

However, it is also important to note that the reduction of surface flow for both perennial and seasonal rivers in the LCB is also compounded by climate and environmental changes. This is confirmed by a recent study by LCBC (2016), which affirms that an increase in the lake area could be a result of no major ongoing irrigation scheme around the Northern pool. This is also reported in Nilsson *et al.* (2016) and Buma *et al.* (2018). This partly confirms the role of surface water abstraction on the lake's water balance.

4.3. Rainfall controls on surface water extent and dynamics

This study found a 4- to 5-month lag of Lake Chad surface water extent to regional rainfall of the contributing basin (Figures 13 and 14). This is in line with the findings of Gbetkom *et al.* (2023) who found a time lag of approximately 112 days between rainfall and Lake Chad water variations. Similarly, Pham-Duc *et al.* (2020) reported a 1-month lag between the peak of the Chari-Logone rivers and the peak of Lake Chad surface water. Zhu *et al.* (2017) reported a time lag of 1–2 months response of streamflow to precipitation in the LCB. As a result, most of the discharge is observed from July to December with a peak value in October (Zhu *et al.* 2017), thus explaining the cycle of the natural lakes in the basin (Figures 2–5, 9 and 12). Lemoalle & Magrin (2014) emphasized that despite surface water abstraction in the LCB, the balance of surface water in Lake Chad is largely explained by precipitation changes. Lemoalle & Magrin (2014) observed that a variation of $\pm 10\%$ in rainfall over the basin corresponds to a variation of the same magnitude of $\pm 30\%$ of the annual flow of river Chari, the main tributary of Lake Chad. Since the surface water of the lake is approximately proportional to the contributions of the Chari River, the surface water extent of the lake is particularly sensitive to variations in precipitation (Lemoalle & Magrin 2014; Mahamat Nour *et al.* 2021; Gbetkom *et al.* 2023).

The LCB shows a succession of wet (excess) and dry (deficit) years which is also reflected in surface water cycles (Figure 14). Though our study did not find a trend in the ERA5-Land precipitation time series, some studies Okonkwo *et al.* 2014; Zhu *et al.* 2017; Buma *et al.* 2018; Dan'azumi & Ibrahim 2023; Gbetkom *et al.* 2023) have reported a slight increase in rainfall in recent years over the LCB. The slight increase in lake area is in line with the findings of Buma *et al.* (2018) which showed improving wet conditions (Figure 14) in the last two decades. The slow recovery rate of Lake Chad has been confirmed by a previous study (Buma *et al.* 2018) applying remote sensing methods. Our findings showed that Lake Chad had an annual average increase rate of 28.54 km^2 following two phases, a low phase between 2003 and 2012 (2,275 km^2) and a high phase from 2013 to 2022 (2,745 km^2) (Figure 11, Supplementary material, Table S1), also confirmed by Buma *et al.* (2018). However, these changing phases of Lake Chad's surface water extent have been reported since the 1920s (Tilho 1928). For 60 years, Lake Chad has oscillated between three stages (small, average, and large Lake Chad), covering a surface water area of around 2,000 to 2,500 km^2 (Magrin *et al.* 2015). The current assessment period shows that Lake Chad exists as '*small Lake Chad*', with varying levels of the Northern pool.

Besides rainfall controls on the hydrological balance of the LCB, underground water flows also play a vital role. Groundwater recharge also contributes to the lake's waters. Diffuse and focus recharge processes have been reported for the Chari-Logone Basin and its wetlands (e.g. Vassolo *et al.* 2016; Bouchez *et al.* 2019). Meanwhile, this was found impossible in the Komadugu-Yobe Basin as a result of clay layers beneath the river Yobe floodplain inhibiting focused recharge (Carter & Alkali 1996). Within the year, the surface water extent in Lake Chad is also partly maintained by groundwater. Vassolo *et al.* (2023) reported a high groundwater concentration along the Lake Chad shore and the Bahr el Ghazal corridor.

5. CONCLUSIONS

In this study, we reconstructed the daily and seasonal cycles of 12 open waterbodies in the LCB between 2003 and 2022 using the GWP. We also verified the relationship between basin-scale precipitation and surface water extent. Several methods including time series decomposition, trend analysis, and change point detection were used. We summarized the main findings as follows;

- A strong seasonality of the natural lakes was observed compared to man-made reservoirs/dams.
- Open water bodies either exhibit a monotonic or cyclic pattern.
- Several phases of dwindling and recovery were identified for Lake Chad, though for the entire study period the lake is recovering at a rate of 28.54 km^2/year.
- In Lake Chad, the maximum water area in all the pools is observed between December and January and the inter-seasonal surface water area varies between ~1,500 and ~3,800–4,000 km^2.
- The Southern pool shows a high water area above 2,400 km^2 at the start and end of each year with the exception of drought years (2006–2017). For wet years (2004, 2018–2022), water area between days 1 and ~ 66, and between 301 and 365/366 days range between 2,200 and ~2,400 km^2. Except for extremely dry years, the water area between the rest of 67–300 days of the year is between 1,600 and 2,000 km^2.
- In contrast, the Northern pool's maximum water area ranges between 1,600 and ~1,700 km^2. With the exception of 2004, 2012, 2013, 2015, 2020, and 2021, the Northern pool only fluctuates between ≤200 and ~800 km^2, staying only for a few days of the year.
- Mean annual water coverage in Lake Chad varied from 2,952.85 to 3,114.43 km^2 between 2004 and 2021, respectively. Meanwhile, between 2005 and 2012 and 2016 and 2019, the surface water area is below 2,500 km^2.
- While the Southern pool remains quasi-stable, the Northern pool shows recovery and dwindling phases, synonym to the historic '*small Lake Chad*'.
- Lake Fitri also depicted marked seasonality but showed a much slower recovery of 1.095 km^2/year.
- In Lake Fitri, surface water showed to stay for a short part of the year, with a peak between 1st and 59th day and between 305th and 365/366th day of the year, while between the 60th and 304th/year (about eight months), the lake exists in a shallow state.
- The recent recovery of Lake Chad has been widely reported, and this is partly linked to recent increases in rainfall over the basin and a reduction in surface water abstraction for irrigation around the Northern portion of the lake.
- The current recovery trend of Lake Chad shows no certainty for stability as this is simply exhibiting the normal but usual cycles of present-day Lake Chad.
- In the sub-humid part of LCB, surface water in Lake Iro stays for 365/366 days/year, but showed a declining trend.
- On the contrary, reservoirs/dams respond to human controls of infilling and withdrawals of water for diverse uses.
- Despite this, a contrast exists between reservoirs/dams. In Northern Nigeria, while the surface water area in Tiga Dam remained quasi-stable, the Challawa Dam reflected extreme hydrological deficit, with a considerable shrinking of dam water area between 2004 and 2006, and between 2014 and 2020.
- In Sahelian Northern Cameroon, the Maga Dam between 2003 and 2010 was quite stable, then strong seasonality set in from 2010 to 2022, and declining area coverage between 2013 and 2019 was observed.

Our study provides additional insights for sustainable water management in LCB in line with FAO's recommendations and targets for the basin. As a response action to the water crisis in the region, FAO (2021) recommended mapping of existing resourceful features around the LCB (Buma *et al.* 2018), including land and water use at cross-border levels. This will assist in addressing the needs of the population with rising food insecurity in the region. Besides, some further research directions include but are not limited to:

- Estimation of surface water extent and dynamics from hyperspectral and microwave sensors may provide an increased understanding of the basin's hydrological cycle.
- Estimation of surface water quality and seasonal concentration of water quality parameters using hyperspectral remote sensing
- Incorporating remote sensing data and future climate models to predict future water variations in the LCB under different climate scenarios.
- Investigating the link between seasonal surface water variations and recurrent land use and armed conflicts in the basin.

ACKNOWLEDGEMENTS

We thank the German Aerospace Center (DLR) – German Remote Sensing Data Center (DFD) for providing the research infrastructure for realizing this study. We appreciate that MODIS data (from which the Global WaterPack is derived) from the National Aeronautics and Space Administration (NASA), ESA WorldCover of European Space Agency (ESA), and the ERA5-Land reanalysis dataset of the European Centre for Medium-Range Weather Forecasts (ECMWF) hosted at climate data store were provided free of charge. We would like to thank Professor Djangrang Man-Na, University of Moundou, Chad for providing *in situ* field observations of the seasonal situation of Lake Fitri. We gratefully thank the anonymous reviewers for their helpful and constructive critiques.

FUNDING

The research was supported by the Alexander von Humboldt Foundation through the International Climate Protection Fellowship.

DATA AVAILABILITY STATEMENT

All relevant data are available from an online repository or repositories. The datasets used in this paper are open source. GWP can be accessed at https://download.geoservice.dlr.de/GWP/files/, JRC surface water product is accessible at https://developers.google.com/earth-engine/datasets/catalog/JRC_GSW1_4_YearlyHistory and ERA5-Land dataset is accessible at https://developers.google.com/earth-engine/datasets/catalog/ECMWF_ERA5_LAND_DAILY_AGGR.

CONFLICT OF INTEREST

The authors declare there is no conflict.

REFERENCES

Abba Umar, D., Ramli, M. F., Tukur, A. I., Jamil, N. R. & Zaudi, M. A. 2021 Detection and prediction of land use change impact on the streamflow regime in Sahelian River Basin, northwestern Nigeria. *H2Open Journal* **4** (1), 92–113. https://doi.org/10.2166/h2oj.2021.065.

Babagana, A., Dungus, B., Bello, S. A. & Kolo, B. 2015 Problems and prospects of Alau Dam construction in Alau community, Konduga local government area, Borno State, Nigeria. *European Scientific Journal, ESJ* **11** (20), 194–207. Available from: https://eujournal.org/index.php/esj/article/view/5961.

Bader, J.-C., Lemoalle, J. & Leblanc, M. 2011 Modèle hydrologique du Lac Tchad. *Hydrological Sciences Journal* **56** (3), 411–425. https://doi.org/10.1080/02626667.2011.560853.

Bdliya, D. H. H. & Bloxom, M. 2007 Transboundary diagnostic analysis of the Lake Chad Basin. Prepared for the LCBC - GEF Project on the Reversal of Land and Water Resources Degradation. Lake Chad Basin Commission (LCBC), N'djamena, Republic of Chad. Available from: http://lakechad.iwlearn.org/publications/reports/lake-cha-basin-tda-report-english (accessed 11 September 2024).

Beck, H. E., McVicar, T. R., Vergopolan, N., Berg, A., Lutsko, N. J., Dufour, A., Zeng, Z., Jiang, X., van Dijk, A. I. J. M. & Miralles, D. G. 2023 High-resolution (1 km) Köppen-Geiger maps for 1901–2099 based on constrained CMIP6 projections. *Scientific Data* **10** (1), 724. https://doi.org/10.1038/s41597-023-02549-6.

BGR n.d *TC Lake Chad Basin: Groundwater Management*. Available from: https://www.bgr.bund.de/EN/Themen/Wasser/Projekte/abgeschlossen/TZ/Tschad/tschad-II_fb_en.html;jsessionid=B7C64632054B76D2A0B961CCD30B5FBD.internet981?nn=1549142 (accessed 7 March 2024).

Birkett, C. M. 2000 Synergistic remote sensing of Lake Chad: Variability of basin inundation. *Remote Sensing of Environment* **72** (2), 218–236. https://doi.org/10.1016/S0034-4257(99)00105-4.

Bonnema, M., David, C. H., Frasson, R. P. d. M., Oaida, C. & Yun, S.-H. 2022 The global surface area variations of lakes and reservoirs as seen from satellite remote sensing. *Geophysical Research Letters* **49** (15), e2022GL098987. https://doi.org/10.1029/2022GL098987.

Bouchez, C., Deschamps, P., Goncalves, J., Hamelin, B., Nour, A. M., Vallet-Coulomb, C. & Sylvestre, F. 2019 Water transit time and active recharge in the Sahel inferred by bomb-produced 36cl. *Scientific Reports* **9**. https://doi.org/10.1038/s41598-019-43514-x.

Buma, W. G., Lee, S.-I. & Seo, J. Y. 2018 Recent surface water extent of Lake Chad from multispectral sensors and GRACE. *Sensors* **18** (7), 2082. https://doi.org/10.3390/s18072082.

Candela, L., Elorza, F. J., Tamoh, K., Jiménez-Martínez, J. & Aureli, A. 2014 Groundwater modelling with limited data sets: The Chari–Logone area (Lake Chad Basin, Chad). *Hydrological Processes* **28** (11), 3714–3727. https://doi.org/10.1002/hyp.9901.

Carter, R. C. & Alkali, A. G. 1996 Shallow groundwater in the northeast arid zone of Nigeria. *Quarterly Journal of Engineering Geology* **29** (4), 341–355. https://doi.org/10.1144/GSL.QJEGH.1996.029.P4.07.

Chiroma, M. J., Kazaure, Y. D., Karaye, Y. B. & Gashua, A. J. 2005 Water management issues in the Hadejia-Jama'are-Komadugu-Yobe Basin: DFID-JWL and stakeholders experience in information sharing, reaching consensus and physical interventions. In *Conference Papers*. Available from: https://ideas.repec.org//p/iwt/conppr/h041158.html (accessed 26 Februay 2024).

Christine, R., Tashi, Y., Jean-François, C., Muriel, B.-N., Mathieu, S. & Florence, S. 2021 Anticipating the evolution of the Fitri lake system: Temporalities of an overflowing flood and its socio-ecological consequences. In *EGU21-14459*. https://doi.org/10.5194/egusphere-egu21-14459.

Chukwuka, O., Emeka, I., Ibrahim, Y., Fenetahun, Y., Yuan, Y. & Yongdong, W. 2023 Remote sensing approach in evaluating anthropogenic impacts on the spatiotemporal changes in net primary productivity of the Niger River Basin, from 2000 to 2020. *Heliyon* **9** (11), e21246. https://doi.org/10.1016/j.heliyon.2023.e21246.

Coe, M. T. & Birkett, C. M. 2004 Calculation of river discharge and prediction of lake height from satellite radar altimetry: Example for the Lake Chad Basin. *Water Resources Research* **40** (10). https://doi.org/10.1029/2003WR002543.

Dan'azumi, S. & Ibrahim, U. A. 2023 Trend analysis of observed precipitation, temperature, and streamflow for Hadejia-Nguru wetlands catchment, Nigeria. *Theoretical and Applied Climatology* **151** (1), 195–207. https://doi.org/10.1007/s00704-022-04270-7.

De Zborowski, I. & Lemoalle, J. 1996 Les surfaces en eau du Lac Tchad: Un suivi par télédétection. In: *Atlas D'élevage du Bassin du Lac Tchad*. Available from: https://agritrop.cirad.fr/590734/ (accessed 26 February 2024).

Djimadoumngar, K.-N. & Adegoke, J. 2018 Satellite-based assessment of land use and land cover (LULC) changes around lake Fitri, Republic of Chad. *Journal of Sustainable Development* **11**, 71. https://doi.org/10.5539/jsd.v11n5p71.

Dubovyk, O., Menz, G., Conrad, C., Kan, E., Machwitz, M. & Khamzina, A. 2013 Spatio-temporal analyses of cropland degradation in the irrigated lowlands of Uzbekistan using remote-sensing and logistic regression modeling. *Environmental Monitoring and Assessment* **185** (6), 4775–4790. https://doi.org/10.1007/s10661-012-2904-6.

Eisfelder, C., Asam, S., Hirner, A., Reiners, P., Holzwarth, S., Bachmann, M., Gessner, U., Dietz, A., Huth, J., Bachofer, F. & Kuenzer, C. 2023 Seasonal vegetation trends for Europe over 30 years from a novel normalised Difference Vegetation Index (NDVI) time-series – the TIMELINE NDVI product. *Remote Sensing* **15** (14), 3616. https://doi.org/10.3390/rs15143616.

Ekpetere, K., Abdelkader, M., Ishaya, S., Makwe, E. & Ekpetere, P. 2023 Integrating satellite imagery and ground-based measurements with a machine learning model for monitoring lake dynamics over a semi-arid region. *Hydrology* **10** (4), 78. https://doi.org/10.3390/hydrology10040078.

European Union, Copernicus Programme 2021 *Copernicus Digital Elevation Model (DEM30)*. Available from: https://developers.google.com/earth-engine/datasets/catalog/COPERNICUS_DEM_GLO30 (accessed 20 December 2023).

FAO 2009 *Adaptive Water Management in the Lake Chad Basin Addressing Current Challenges and Adapting to Future Needs*. Available from: https://www.fao.org/fileadmin/user_upload/faowater/docs/ChadWWW09.pdf (accessed 7 March 2024).

FAO 2021 *Evaluation of the FAO Response to the Crisis in the Lake Chad Basin 2015–2018*. Programme evaluation series, January 2021. Food and Agriculture Organization of the United Nations, Rome. Available from: https://www.fao.org/documents/card/en?details=CB3138EN/ (accessed 7 March 2024).

Fu, S., Zhou, Y., Lei, J. & Zhou, N. 2023 Changes in the spatiotemporal of net primary productivity in the conventional Lake Chad Basin between 2001 and 2020 based on CASA model. *Atmosphere* **14** (2), 232. https://doi.org/10.3390/atmos14020232.

Gao, H., Bohn, T. J., Podest, E., McDonald, K. C. & Lettenmaier, D. P. 2011 On the causes of the shrinking of lake Chad. *Environmental Research Letters* **6** (3), 034021. https://doi.org/10.1088/1748-9326/6/3/034021.

Gbetkom, P. G., Crétaux, J.-F., Tchilibou, M., Carret, A., Delhoume, M., Bergé-Nguyen, M. & Sylvestre, F. 2023 Lake Chad vegetation cover and surface water variations in response to rainfall fluctuations under recent climate conditions (2000 – 2020). *Science of the Total Environment* **857**, 159302. https://doi.org/10.1016/j.scitotenv.2022.159302.

Gbode, I. E., Babalola, T. E., Diro, G. T. & Intsiful, J. D. 2023 Assessment of ERA5 and ERA-Interim in reproducing mean and extreme climates over West Africa. *Advances in Atmospheric Sciences* **40** (4), 570–586. https://doi.org/10.1007/s00376-022-2161-8.

Geerken, R., Vassolo, S., Bila, M., 2012 Impacts of climate variability and population pressure on water resources in the Lake Chad Basin. River Basins and Change. In: *Conference of the Global Catchment Initiative (GCI), The Global Dimensions of Change in River Basins* (Bogardi, J. J., Leentvaar, J. & Nachtnebel, H.-P., eds). Bundesanstalt für Geowissenschaften und Rohstoffe (BGR), Bonn, Germany, pp. 27–33.

GIZ 2018 *Transboundary Diagnostic Analysis of the Lake Chad Basin – 2018 Update*. Available from: https://iwlearn.net/documents/32059 (accessed 7 March 2024).

Global Water Partnership 2013 *The Lake Chad Basin Aquifer System*. Available from: https://www.gwp.org/globalassets/global/toolbox/references/lake_chad_fact_sheet.pdf (accessed 7 March 2024).

Goni, I. B., Taylor, R. G., Favreau, G., Shamsudduha, M., Nazoumou, Y. & Ngounou, N. B. 2021 Groundwater recharge from heavy rainfall in the southwestern Lake Chad Basin: Evidence from isotopic observations. *Hydrological Sciences Journal* **66** (8), 1359–1371. https://doi.org/10.1080/02626667.2021.1937630.

Gorelick, N., Hancher, M., Dixon, M., Ilyushchenko, S., Thau, D. & Moore, R. 2017 Google earth engine: Planetary-scale geospatial analysis for everyone. *Remote Sensing of Environment*. **202**, 18–27. https://doi.org/10.1016/j.rse.2017.06.031.

Goswami, M. M., Mujumdar, M., Singh, B. B., Ingale, M., Ganeshi, N., Ranalkar, M., Franz, T. E., Srivastav, P., Niyogi, D., Krishnan, R. & Patil, S. N. 2023 Understanding the soil water dynamics during excess and deficit rainfall conditions over the core monsoon zone of India. *Environmental Research Letters* **18** (11), 114011. https://doi.org/10.1088/1748-9326/acffdf.

Goudiaby, O., Bodian, A., Dezetter, A., Diouf, I. & Ogilvie, A. 2024 Evaluation of gridded rainfall products in three West African basins. *Hydrology* **11** (6), 75. https://doi.org/10.3390/hydrology11060075.

GWSP IPO 2012 River basins and change conference of the global catchment initiative (GCI). In *The Global Dimensions of Change in River Basins*, p. 206.

Hamed, K. H. & Ramachandra Rao, A. 1998 A modified Mann-Kendall trend test for autocorrelated data. *Journal of Hydrology* **204** (1), 182–196. https://doi.org/10.1016/S0022-1694(97)00125-X.

Hansen, K. 2017 *The Rise and Fall of Africa's Great Lake: Scientists Try to Understand the Fluctuations of Lake Chad*. Available from: https://earthobservatory.nasa.gov/features/LakeChad (accessed 26 February 2024).

Herndon, K., Muench, R., Cherrington, E. & Griffin, R. 2020 An assessment of surface water detection methods for water resource management in the Nigerien Sahel. *Sensors* **20** (2), 431. https://doi.org/10.3390/s20020431.

Huang, C., Chen, Y., Zhang, S. & Wu, J. 2018 Detecting, extracting, and monitoring surface water from space using optical sensors: A review. *Reviews of Geophysics* **56** (2), 333–360. https://doi.org/10.1029/2018RG000598.

Hussain, M. M. & Mahmud, I. 2019 Pymannkendall: A python package for non parametric Mann Kendall family of trend tests. *Journal of Open Source Software* **4** (39), 1556. https://doi.org/10.21105/joss.01556.

Hussain, M. M., Mahmud, I. & Bari, S. H. 2023 Pyhomogeneity: A Python package for homogeneity test of time series data. *Journal of Open Source Software* **11** (1), 4. https://doi.org/10.5334/jors.427.

Kendall, M. G. 1948 *Rank Correlation Methods*. Griffin, London.

Klein, I., Dietz, A. J., Gessner, U., Galayeva, A., Myrzakhmetov, A. & Kuenzer, C. 2014 Evaluation of seasonal water body extents in Central Asia over the past 27 years derived from medium-resolution remote sensing data. *International Journal of Applied Earth Observation and Geoinformation* **26**, 335–349. https://doi.org/10.1016/j.jag.2013.08.004.

Klein, I., Dietz, A., Gessner, U., Dech, S. & Kuenzer, C. 2015 Results of the global waterPack: A novel product to assess inland water body dynamics on a daily basis. *Remote Sensing Letters* **6** (1), 78–87. https://doi.org/10.1080/2150704X.2014.1002945.

Klein, I., Gessner, U., Dietz, A. J. & Kuenzer, C. 2017 Global waterPack – a 250m resolution dataset revealing the daily dynamics of global inland water bodies. *Remote Sensing of Environment* **198**, 345–362. https://doi.org/10.1016/j.rse.2017.06.045.

Klein, I., Gessner, U., Dietz, A. & Kuenzer, C. 2021a *Global WaterPack – MODIS – Daily*. Available from: https://doi.org/10.15489/vcalr2s1qv66.

Klein, I., Mayr, S., Gessner, U., Hirner, A. & Kuenzer, C. 2021b Water and hydropower reservoirs: High temporal resolution time series derived from MODIS data to characterize seasonality and variability. *Remote Sensing of Environment* **253**, 112207. https://doi.org/10.1016/j.rse.2020.112207.

Klein, I., Uereyen, S., Sogno, P., Twele, A., Hirner, A. & Kuenzer, C. 2024 Global waterPack – the development of global surface water over the past 20 years at daily temporal resolution. *Scientific Data* **11** (1), 472. https://doi.org/10.1038/s41597-024-03328-7.

Köppen, W. 1900 Versuch einer klassifikation der klimate, vorzugsweise nach ihren beziehungen zur pflanzenwelt. *Geographische Zeitschrift* **6** (11), 593–611. Available from: https://www.jstor.org/stable/27803924 (accessed 27 July 2024).

Lake Chad Basin Commission 2016 *The Lake Chad Development and Climate Resilience Action Plan*. World Bank, Washington, DC. https://doi.org/10.1596/23793 (accessed 3 July 2024).

Lemenkova, P. 2023 Using open-source software GRASS GIS for analysis of the environmental patterns in Lake Chad, Central Africa. *Journal of Land Management, Food and Environment* **74** (1), 49–64. Available from: https://sciendo.com/article/10.2478/boku-2023-0005.

Lemoalle, J. 2004 Lake Chad: A changing environment. In: *Dying and Dead Seas Climatic Versus Anthropic Causes, NATO Science Series: IV: Earth and Environmental Sciences* (Nihoul, J. C. J., Zavialov, P. O. & Micklin, P. P., eds). Springer Netherlands, Dordrecht, pp. 321–339. https://doi.org/10.1007/978-94-007-0967-6_13.

Lemoalle, J. & Magrin, G. 2014 *Le Développement du lac Tchad: Situation Actuelle et Futurs Possibles, Collection Expertise Collégiale*. IRD éditions, Marseille.

Li, L., Vrieling, A., Skidmore, A. & Wang, T. 2020 Evaluation of a new 18-year MODIS-derived surface water fraction dataset for constructing Mediterranean wetland open surface water dynamics. *Journal of Hydrology* **587**, 124956. https://doi.org/10.1016/j.jhydrol.2020.124956.

Ling, F., Li, X., Foody, G. M., Boyd, D., Ge, Y., Li, X. & Du, Y. 2020 Monitoring surface water area variations of reservoirs using daily MODIS images by exploring sub-pixel information. *ISPRS Journal of Photogrammetry and Remote Sensing* **168**, 141–152. https://doi.org/10.1016/j.isprsjprs.2020.08.008.

Liu, Y., Liu, R. & Shang, R. 2022 GLOBMAP SWF: A global annual surface water cover frequency dataset during 2000–2020. *Earth System Science Data* **14** (10), 4505–4523. https://doi.org/10.5194/essd-14-4505-2022.

Magrin, G., Lemoalle, J. & Pourtier, R. 2015 *Atlas du lac Tchad*. Passages. Available form: https://hal.science/hal-01237595 (accessed 1 March 2024).

Mahamat Nour, A., Vallet-Coulomb, C., Gonçalves, J., Sylvestre, F. & Deschamps, P. 2021 Rainfall-discharge relationship and water balance over the past 60 years within the Chari-Logone sub-basins, Lake Chad Basin. *Journal of Hydrology: Regional Studies* **35**, 100824. https://doi.org/10.1016/j.ejrh.2021.100824.

Mann, H. B. 1945 Mann: Nonparametric tests against trend. *Econometrica* **13** (3), 245–259. doi: 10.2307/1907187.

Messager, M. L., Lehner, B., Grill, G., Nedeva, I. & Schmitt, O. 2016 Estimating the volume and age of water stored in global lakes using a geo-statistical approach. *Nature Communications* **7** (1), 13603. https://doi.org/10.1038/ncomms13603.

Militino, A. F., Moradi, M. & Ugarte, M. D. 2020 On the performances of trend and change-point detection methods for remote sensing data. *Remote Sensing* **12** (6), 1008. https://doi.org/10.3390/rs12061008.

Mueller, N., Lewis, A., Roberts, D., Ring, S., Melrose, R., Sixsmith, J., Lymburner, L., McIntyre, A., Tan, P., Curnow, S. & Ip, A. 2016 Water observations from space: Mapping surface water from 25 years of Landsat imagery across Australia. *Remote Sensing of Environment* **174**, 341–352. https://doi.org/10.1016/j.rse.2015.11.003.

Muñoz-Sabater, J., Dutra, E., Agustí-Panareda, A., Albergel, C., Arduini, G., Balsamo, G., Boussetta, S., Choulga, M., Harrigan, S., Hersbach, H., Martens, B., Miralles, D. G., Piles, M., Rodríguez-Fernández, N. J., Zsoter, E., Buontempo, C. & Thépaut, J.-N. 2021 ERA5-land: A state-of-the-art global reanalysis dataset for land applications. *Earth System Science Data* **13** (9), 4349–4383. https://doi.org/10.5194/essd-13-4349-2021.

Nilsson, E., Hochrainer-Stigler, S., Mochizuki, J. & Uvo, C. B. 2016 Hydro-climatic variability and agricultural production on the shores of Lake Chad. *Environmental Development* **20**, 15–30. https://doi.org/10.1016/j.envdev.2016.09.001.

Okonkwo, C., Demoz, B. & Gebremariam, S. 2014 Characteristics of Lake Chad level variability and links to ENSO, precipitation, and river discharge. *The Scientific World Journal* **2014**, e145893. https://doi.org/10.1155/2014/145893.

Olivry, J.-C. 1996 *Hydrologie du Lac Tchad, Monographies Hydrologiques*. ORSTOM éditions, Paris.

Olowoyeye, O. S. & Kanwar, R. S. 2023 Water and food sustainability in the Riparian countries of Lake Chad in Africa. *Sustainability* **15** (13), 10009. https://doi.org/10.3390/su151310009.

Parajuli, B., Zhang, X., Deuja, S. & Liu, Y. 2021 Regional and seasonal precipitation and drought trends in Ganga–Brahmaputra basin. *Water* **13** (16), 2218. https://doi.org/10.3390/w13162218.

Pattnayak, K. C., Abdel-Lathif, A. Y., Rathakrishnan, K. V., Singh, M., Dash, R. & Maharana, P. 2019 Changing climate over Chad: Is the rainfall over the major cities recovering? *Earth and Space Science* **6** (7), 1149–1160. https://doi.org/10.1029/2019EA000619.

Pekel, J.-F., Cottam, A., Gorelick, N. & Belward, A. S. 2016 High-resolution mapping of global surface water and its long-term changes. *Nature* **540** (7633), 418–422. https://doi.org/10.1038/nature20584.

Pettitt, A. N. 1979 A non-parametric approach to the change-point problem. *Journal of the Royal Statistical Society. Series C (Applied Statistics)* **28** (2), 126–135. https://doi.org/10.2307/2346729.

Pham-Duc, B., Sylvestre, F., Papa, F., Frappart, F., Bouchez, C. & Crétaux, J.-F. 2020 The Lake Chad hydrology under current climate change. *Scientific Reports* **10** (1), 5498. https://doi.org/10.1038/s41598-020-62417-w.

Pickens, A. H., Hansen, M. C., Hancher, M., Stehman, S. V., Tyukavina, A., Potapov, P., Marroquin, B. & Sherani, Z. 2020 Mapping and sampling to characterize global inland water dynamics from 1999 to 2018 with full landsat time-series. *Remote Sensing of Environment* **243**, 111792. https://doi.org/10.1016/j.rse.2020.111792.

Poulin, C., Hamelin, B., Vallet-Coulomb, C., Amngar, G., Loukman, B., Cretaux, J.-F., Doumnang, J.-C., Mahamat Nour, A., Menot, G., Sylvestre, F. & Deschamps, P. 2019 Unraveling the hydrological budget of isolated and seasonally contrasted subtropical lakes. *Hydrology and Earth System Sciences* **23** (3), 1705–1724. https://doi.org/10.5194/hess-23-1705-2019.

Quagraine, K. A., Nkrumah, F., Klein, C., Klutse, N. A. B. & Quagraine, K. T. 2020 West African summer monsoon precipitation variability as represented by reanalysis datasets. *Climate* **8** (10), 111. https://doi.org/10.3390/cli8100111.

Saley, I. A. & Salack, S. 2023 Present and future of heavy rain events in the Sahel and West Africa. *Atmosphere* **14** (6), 965. https://doi.org/10.3390/atmos14060965.

Sanni, M. I. 2018 *Geographical information system based hydrological modelling of climate change variables on Hadejia river sub-basin*. PhD dissertation. Ahmadu Bello University, Zaria, Nigeria

Savitzky, A. & Golay, M. J. E. 1964 Smoothing and differentiation of data by simplified least squares procedures. *Analytical Chemistry* **36** (8), 1627–1639. https://doi.org/10.1021/ac60214a047.

Sen, P. K. 1968 Estimates of the regression coefficient based on Kendall's tau. *Journal of the American Statistical Association* **63** (324), 1379–1389. doi:10.1080/01621459.1968.10480934.

Talikun, T., Raimond, C., Nagorngar, A. K., Zakinet, D., Schuster, M., Sylvestre, F., 2019 Variabilité des crues et des paysages du lac Fitri depuis les grandes sécheresses des années 1970–1980. In: *Le Tchad des Lacs: Les Zones Humides Sahéliennes au Défi du Changement Global (Variability of Floods and Landscapes of Lake Fitri Since the Great Droughts of the 1970s-1980s* (Raimond, C., Sylvestre, F., Zakinet, D. & Moussa, A., eds) The Chad of the lakes: Sahelian wetlands facing the challenge of global change), IRD Editions. ed. Institut de Recherche pour le Développement, Marseille.

Theil, H. 1950 *A Rank-Invariant Method of Linear and Polynomial Regression Analysis, 3; Confidence Regions for the Parameters of Polynomial Regression Equations*. Available form: https://ir.cwi.nl/pub/18448.

Thomas, G. A. 2008 *Reoptimization of West African Dams to Restore Downstream Ecosystems & Livelihoods*. Available form: https://www.afdb.org/fileadmin/uploads/afdb/Documents/Generic-Documents/30696763-FR-PARAL-3-2-NHI-THOMAS.PDF (accessed 11 June 2023).

Tilho, J. 1928 Variations et disparition possible du Tchad. *Annales de Géographie* **37** (207), 238–260. https://doi.org/10.3406/geo.1928.9299.

Uereyen, S., Bachofer, F., Klein, I. & Kuenzer, C. 2022 Multi-faceted analyses of seasonal trends and drivers of land surface variables in Indo-Gangetic river basins. *Science of The Total Environment* **847**, 157515. https://doi.org/10.1016/j.scitotenv.2022.157515.

Vaquero, G., Siavashani, N. S., García-Martínez, D., Elorza, F. J., Bila, M., Candela, L. & Serrat-Capdevila, A. 2021 The lake Chad transboundary aquifer. Estimation of groundwater fluxes through international borders from regional numerical modeling. *Journal of Hydrology: Regional Studies* **38**, 100935. https://doi.org/10.1016/j.ejrh.2021.100935.

Vassolo, S., Wilczok, C., Daïra, D. & Bala, A. 2016 *Groundwater – Surface Water Interaction in the Lower Logone Floodplain*. Available form: https://elvis/fsc/fscasp/content/bin/fscvext.dll?mx=COO.2164.100.6.150281.

Vassolo, S., Gröschke, M., Koeniger, P., Neukum, C., Seehausen, L., Witt, L., Ronnelngar, M. & Daïra, D. 2023 Groundwater recharge processes in the Lake Chad Basin based on isotopic and chemical data. *Hydrogeology Journal* **32**, 149–165. https://doi.org/10.1007/s10040-023-02699-2.

Vivekananda Wall, M., Sylvestre, F. & Nagarajan, C. 2019 *Shoring Up Stability: Addressing Climate & Fragility Risks in the Lake Chad Region*. Available form: https://adelphi.de/en/publications/shoring-up-stability (accessed 26 February 2024).

Wald, L. 1990 Monitoring the decrease of Lake Chad from space. *Geocarto International* **5** (3), 31–36. https://doi.org/10.1080/10106049009354266.

Yang, Y., Huang, S., Qiu, J., Liu, C. & Jiang, W. 2022 A surface water mapping framework combining optical and radar remote sensing and its application in China. *Geocarto International* **37** (27), 17547–17564. https://doi.org/10.1080/10106049.2022.2129836.

Yue, S. & Wang, C. 2004 The Mann-Kendall test modified by effective sample size to detect trend in serially correlated hydrological series. *Water Resources Management* **18** (3), 201–218. https://doi.org/10.1023/B:WARM.0000043140.61082.60.

Zanaga, D., Van De Kerchove, R., De Keersmaecker, W., Souverijns, N., Brockmann, C., Quast, R., Wevers, J., Grosu, A., Paccini, A., Vergnaud, S., Cartus, O., Santoro, M., Fritz, S., Georgieva, I., Lesiv, M., Carter, S., Herold, M., Li, L., Tsendbazar, N.-E., Ramoino, F. & Arino, O. 2021 *ESA WorldCover 10 M 2020 v100*. https://doi.org/10.5281/zenodo.5571936.

Zhao, S., Cook, K. H. & Vizy, E. K. 2023 How shrinkage of Lake Chad affects the local climate. *Climate Dynamics* **61** (1), 595–619. https://doi.org/10.1007/s00382-022-06597-3.

Zhou, Y., Dong, J., Xiao, X., Xiao, T., Yang, Z., Zhao, G., Zou, Z. & Qin, Y. 2017 Open surface water mapping algorithms: A comparison of water-related spectral indices and sensors. *Water* **9** (4), 256. https://doi.org/10.3390/w9040256.

Zhu, W., Yan, J. & Jia, S. 2017 Monitoring recent fluctuations of the southern pool of Lake Chad using multiple remote sensing data: Implications for water balance analysis. *Remote Sensing* **9** (10), 1032. https://doi.org/10.3390/rs9101032.

Zilefac, E. A. 2010 *Analysis of Climate Variability and Anthropogenic Impacts on the Water Balance of Lake Chad Drainage Basin*. *Master's Thesis*, Lund University. 60.

First received 28 April 2024; accepted in revised form 12 August 2024. Available online 29 August 2024